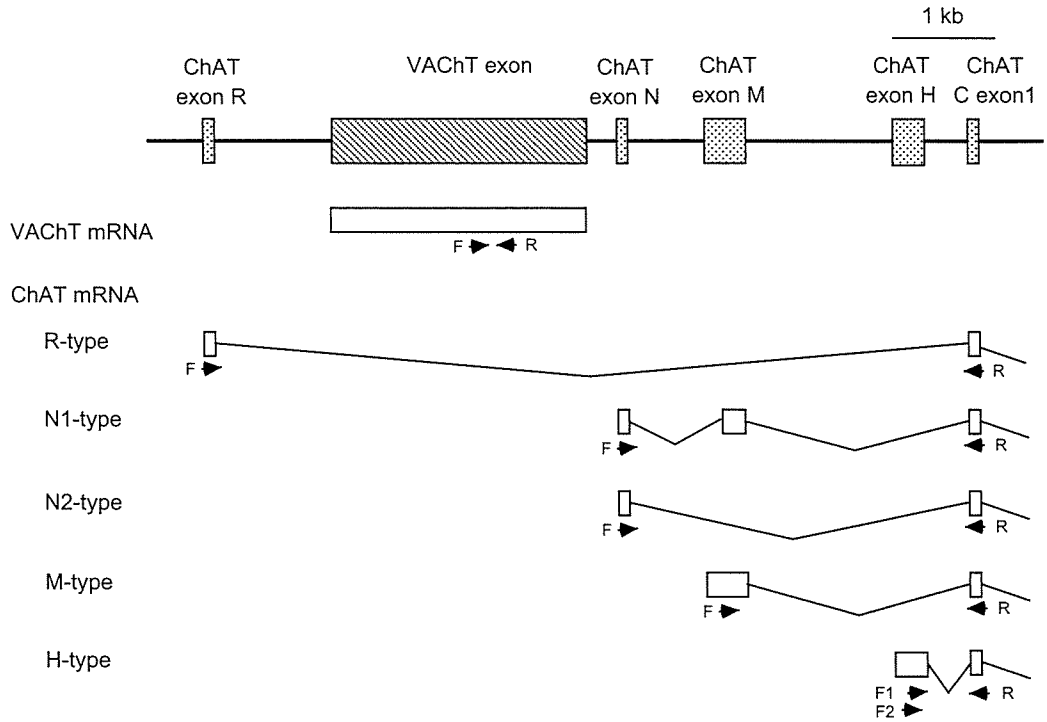

Fig. 1. Schematic representation of the structure of the 5′ region of the human cholinergic gene locus, the splicing patterns of multiple ChAT mRNAs, and the positions of the primers (arrows: F, forward primer; R, reverse primer) shown in Table 1 for PCR analyses. Thirteen common exons of ChAT following the common exon 1 (ChAT C exon 1) are omitted in the figure.

placenta tissue and a set of CoREST F2 and R2 primers; 38-cycle PCR with total RNAs extracted from spinal motor neurons or placental trophoblastic cells and a set of CoREST F2 and R2 primers) were normalized to those of the β-actin bands (25-cycle PCR with total RNAs extracted from spinal cord or placenta tissue; 30-cycle PCR with total RNAs extracted from spinal motor neurons or placental trophoblastic cells). The mean of the REST/NRSE or CoREST ratio values of three spinal cords normalized to the β-actin values were arbitrarily expressed as a fold of 1.

Preparation of a polyclonal antibody to the recombinant human VAChT carboxyl terminus

Construction of the PGEX-5X-1-hVAChT plasmid. A genomic clone for human VAChT (Cos #25) was isolated from a genomic cosmid library constructed with human blood cells (Oda et al., 1992), which contained the entire coding region for VAChT, as reported previously by other researchers (Erickson et al., 1994). The DNA encoding the carboxyl terminus (amino acids 473–532) was subcloned by PCR (Perkin-Elmer/Cetus, Norwalk, CT, USA), using Cos #25 as a template. Forward and reverse primers with mutations were designed to generate *Bam*HI and *Eco*RI, respectively (5′-GCTGCT GCTCCGCAACGTGGGGATCCTGACGCGCTCCCGTTCCG-3′ and 5′-GGTGGGCTGGAGGAGGAGTGGGAATTCTAGCTGCGG-GTGTAGTAGTAG-3′; induced mutations are underlined). The amplified DNA fragments were purified and inserted between the *Bam*HI and *Eco*RI sites of pGEX-5X-1. Recombinant DNAs were sequenced using a terminator cycle sequencing kit (*Taq* DeyDeoxy; Applied Biosystems, Foster City, CA, USA) and a DNA sequencer (Model 377; Applied Biosystems) to confirm that the plasmid with the expected VAChT DNA fragment was successfully cloned.

Expression and isolation of human VAChT carboxyl terminus. The expected protein consisted of 60 amino acids of the human VAChT carboxyl terminus without GST-derived amino acids. The recombinant DNA was expressed in *Escherichia coli* JM105 with 1 mM isopropylthio-β-D-thiogalactoside. Bacteria were lysed by sonication in a PBS buffer. After being extracted by adding Triton X-100 to a final concentration of 1%, the cloned protein was affinity-purified from the bacterial lysates using glutathione sepharose 4B affinity column chromatography (Pharmacia Biotech, U.K.). The human VAChT protein was separated by cleavage with factor Xa. However, the chromatography could not eliminate contaminated the bacterial proteins completely. Thus, the human VAChT carboxyl terminus was further purified by electrophoresis. The cleaved sample was electrophoresed by sodium dodecyl sulfate polyacrylamide gel electrophoresis on 15% acrylamide gel under a reduced condition. The expressed VAChT protein was extracted from the gel with 10 mM Tris–HCl (pH 7.5) containing 0.1% sodium dodecyl sulfate, concentrated with Amicon PM10 (Grace Japan, Tokyo, Japan), and dialyzed against 10 mM sodium hydrogen carbonate. Amino terminal sequencing of the isolated protein was performed with a protein sequencer (N/C Protein Sequencer System HP 241; Yokogawa Analytical Systems, Tokyo, Japan). Finally, the purified protein consisted of 53 amino acids of the VAChT carboxyl terminus, which lacked seven amino acids of the N-terminal, probably because of cleavage during the preparation.

Antibody production. All animal procedures were performed according to Japanese guidelines of the Prime Minister's Office for the care and use of laboratory animals. All efforts were made to minimize the number of animals used and their suffering. A rat was injected intradermally with 0.4 mg of the human VAChT carboxyl terminus emulsified in Freund's complete adjuvant. The animal was boosted three times with 0.2 mg of the protein at 2-week intervals. During immunization, the antibody titer was monitored by ELISA (Voller et al., 1976). The blood was collected by heart puncture 7 days after the last immunization. IgG was

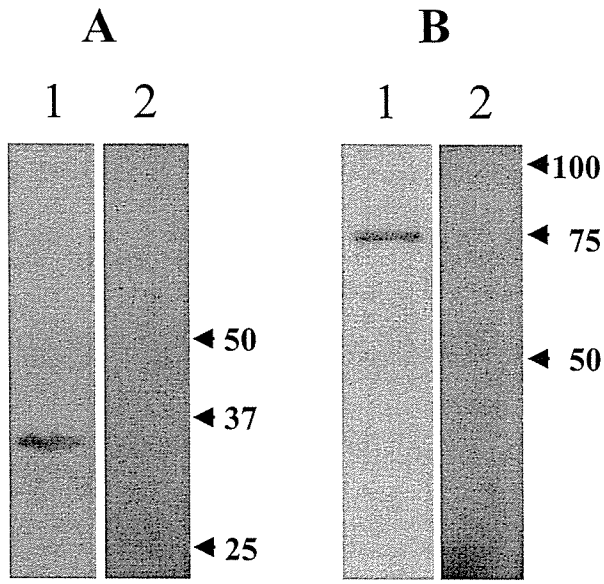

Fig. 2. Evaluation of the specificity of an anti-human VAChT protein antibody by Western blotting before (lane 1) or after (lane 2) preadsorption with 5 μM of purified VAChT C-terminus protein. (A) Lysates of bacteria expressing GST-VAChT fusion protein on 15% polyacrylamide–sodium dodecyl sulfate gel. (B) Homogenates of the human spinal cord on 10% polyacrylamide–sodium dodecyl sulfate gel. Molecular weights are indicated in kDa.

purified from the antiserum with protein A column chromatography.

Western blot analysis. Crude membrane fractions containing VAChT were prepared from the human spinal cord according to the method by Roghani et al. (1998) with some modifications. The spinal cord obtained at autopsy was homogenated in 20 mM Tris–HCl (pH 7.6) with 125 mM NaCl, 5 mM EDTA disodium salt, 5 mM *n*-ethylmaleimide, 2 mM phenylmethylsulfonyl fluoride, 1 mM pepstatin A, and 1 mM leupeptin, and centrifuged for 10 min at 7000×*g* at 4 °C. The supernatants were collected and centrifuged for 20 min at 20,000×*g* at 4 °C. The membrane pellets were obtained from the resulting supernatants by centrifugation for 45 min at 180,000×*g* at 4 °C, and resuspended in cold 0.32 M sucrose, 10 mM HEPES-KOH (pH 7.6), 5 mM EDTA disodium salt, 5 mM *n*-ethylmaleimide, 2 mM phenylmethylsulfonyl fluoride, 1 mM pepstatin A, and 1 mM leupeptin. Thirty micrograms of resuspended protein was electrophoresed on a 10% polyacrylamide–sodium dodecyl sulfate gel under reduction or non-reduction conditions and electrophoretically transferred to a nitrocellulose filter. The filter was blocked by an overnight incubation in phosphate-buffered saline (PBS) containing 2% bovine serum albumin (BSA) at 4 °C, followed by an overnight incubation in PBS containing 2% BSA and a polyclonal antibody against VAChT fusion protein (diluted 1:1000). The filter was washed three times in PBS containing 0.05% Tween-20 (TPBS) for 20 min each time and then incubated with a rabbit anti-rat antibody conjugated with peroxidase (diluted in 1:500; Dako, Glostrup, Denmark) for 1 h at room temperature. After the filter was washed in TPBS, the bound antibody was visualized with a chemiluminescent system (SuperSignal West Dura Extended Duration Substrate; Pierce, Rockford, IL, USA). Control experiments were performed to confirm specificity of the anti-VAChT antibody. For a positive control, 30 μg of lysates of bacteria expressing GST-VAChT fusion protein was electrophoresed on a 15% polyacrylamide–sodium dodecyl sulfate gel and processed with Western blot analysis. For a negative control, the primary antibody was preadsorbed by incubation of the purified VAChT carboxyl terminus protein (5 μM) overnight at 4 °C and centrifuged for 1 h at 10,000×*g* at 4 °C, or was replaced by a normal rat serum.

Immunohistochemistry for ChAT and VAChT

The tissue sections were cut from paraformaldehyde-fixed, paraffin-embedded tissue blocks and mounted on slides coated with poly-L-lysine. The tissue sections were deparaffinized and treated with 1% H_2O_2 for 10 min to quench the endogenous peroxidase activity, followed by microwave treatment to enhance the immunoreactivity. After preincubation with normal goat or rabbit serum diluted 1:10 for 30 min at room temperature, the sections were incubated overnight at 4 °C with a 1:1000 dilution of the polyclonal rabbit antibody against a human ChAT fusion protein (Oda et al., 1995), or a 1:200 dilution of the polyclonal rat antibody against a human VAChT fusion protein. The sections were rinsed three times in 0.02 M PBS for 10 min and reacted with biotinylated goat IgG against rabbit IgG or biotinylated rabbit IgG against rat IgG (diluted 1:200, Dako) for 30 min at room temperature. The tissues were then rinsed in several changes of PBS, followed by incubation with an avidin–biotin–peroxidase complex (Dako) for 30 min. Antibody binding was visualized with 3,3′-diaminobenzidine tetrahydrochloride, and the sections were counterstained with hematoxylin. The sections incubated with non-immune rabbit or rat IgG instead of the primary antibody served as negative reaction controls.

RESULTS

Western blot analysis

In order to verify the recognition ability of the purified immunoglobulin for the human VAChT protein, immunoblot analysis was performed. The antibody was immunoreactive with the GST-VAChT fusion protein expressed in bacteria (Fig. 2A), and an approximately 75 kDa protein in the crude membrane fractions of the spinal cord (Fig. 2B). No immunoreactive bands were observed in the blot membrane incubated with the preadsorbed antibody with the

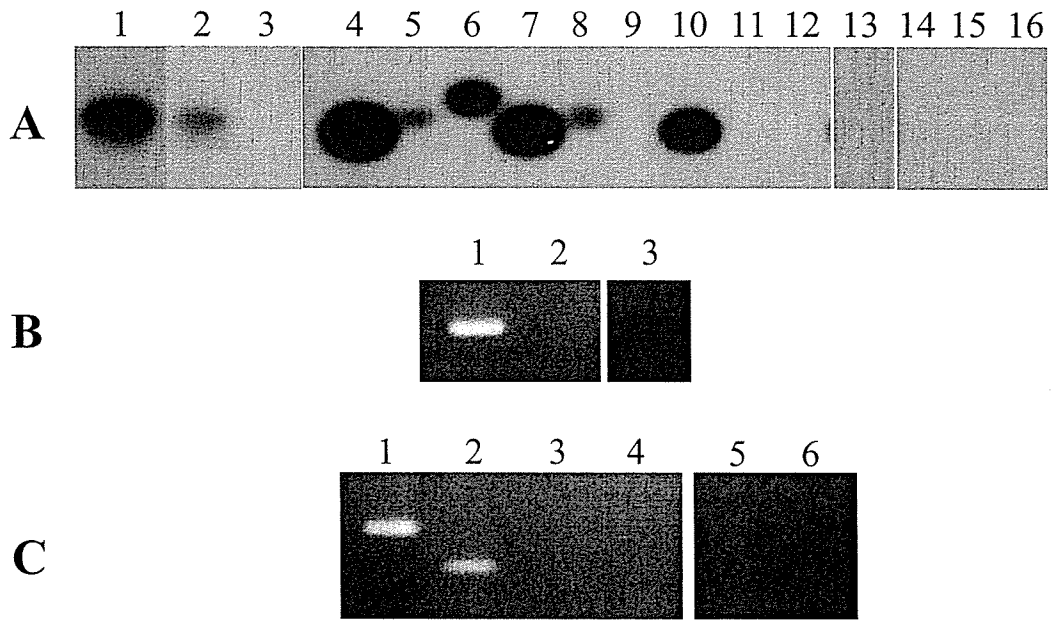

Fig. 3. Expression of ChAT (A), VAChT (B), and CHT1 (C) in the human spinal cord and term placenta. (A) Southern blot analysis following RT-PCR for the detection of H-type (lanes 1, 2, 3, and 13, with a set of forward primer 1 and reverse primer), M-type (lanes 4, 7, 10, and 14), N-type (lanes 5, 8, 11, and 15) and R-type (lanes 6, 9, 12, and 16) mRNAs in tissue of the spinal cord (lanes 1, 4, 5, 6, 13, 14, 15, and 16) and term placenta (lane 2, sample 1; lane 3, sample 2; lanes 7, 8, and 9, sample 3; lanes 10, 11, and 12, sample 4). PCR was done without a step of reverse-transcriptase reaction in lanes 13, 14, 15, and 16 (spinal cord). (B) Agarose-gel electrophoresis of RT-PCR products: lanes 1 and 3, spinal cord; lane 2, term placenta. PCR was done without a step of reverse-transcriptase reaction in lane 3. (C) Agarose-gel electrophoresis of RT-PCR products with a set of forward primer 1 and reverse primer 1 (lanes 1, 3, and 5), and a set of forward primer 2 and reverse primer 2 (lanes 2, 4, and 6): lanes 1, 2, 5 and 6, spinal cord; lanes 3 and 4, term placenta. PCR was done without a step of reverse-transcriptase reaction in lanes 5 and 6.

VAChT carboxyl terminus protein (Fig. 2), or the normal rat serum instead of the antibody raised against the VAChT carboxyl terminus protein.

Detection of ChAT, VAChT, and CHT1

H-type, M-type, N2-type, and R-type ChAT mRNAs, VAChT mRNA, and CHT1 mRNA were amplified by RT-PCR in the autopsied spinal cord (Fig. 3). The relative intensity of the hybridization signal in the Southern blot experiments, using the same ^{32}P-labeled probe, was strongest in the order of M-type, R-type and N2-type, as already reported by Misawa et al. (1997). The expression level of the H-type was slight lower than that of the N2-type (Fig. 4). The M-type ChAT mRNA was detected in all placenta samples, the H-type ChAT mRNA in six placenta samples, and the N2-type ChAT mRNA in three placenta samples. Intensity of the M-type signal was stronger than that of the H-type or N2-type signal in all placenta tissue samples. In one placenta sample with the expression of three types, the relative intensity of the hybridization signal was strongest in the order of M-type, N2-type and H-type. The R-type ChAT, VAChT and CHT1 mRNAs were not detected in any placenta tissue samples. Bands were not observed in the PCR products generated without a step of reverse-transcriptase reaction.

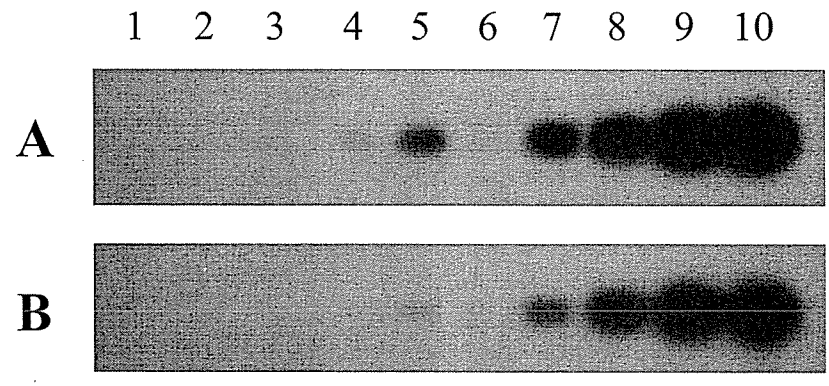

Fig. 4. Semiquantitative PCR analysis of N2-type (A) and H-type (B) mRNAs in the human spinal cord. Lanes 1–5, Southern blot following PCR with mRNA isolated from the spinal cord; lanes 6–10, with 1 pg of the control DNAs. Lanes 1 and 6, PCR for 20 cycles; lanes 2 and 7, for 25 cycles; lanes 3 and 8, for 28 cycles; lanes 4 and 9, 31 cycles; lanes 5 and 10, 34 cycles.

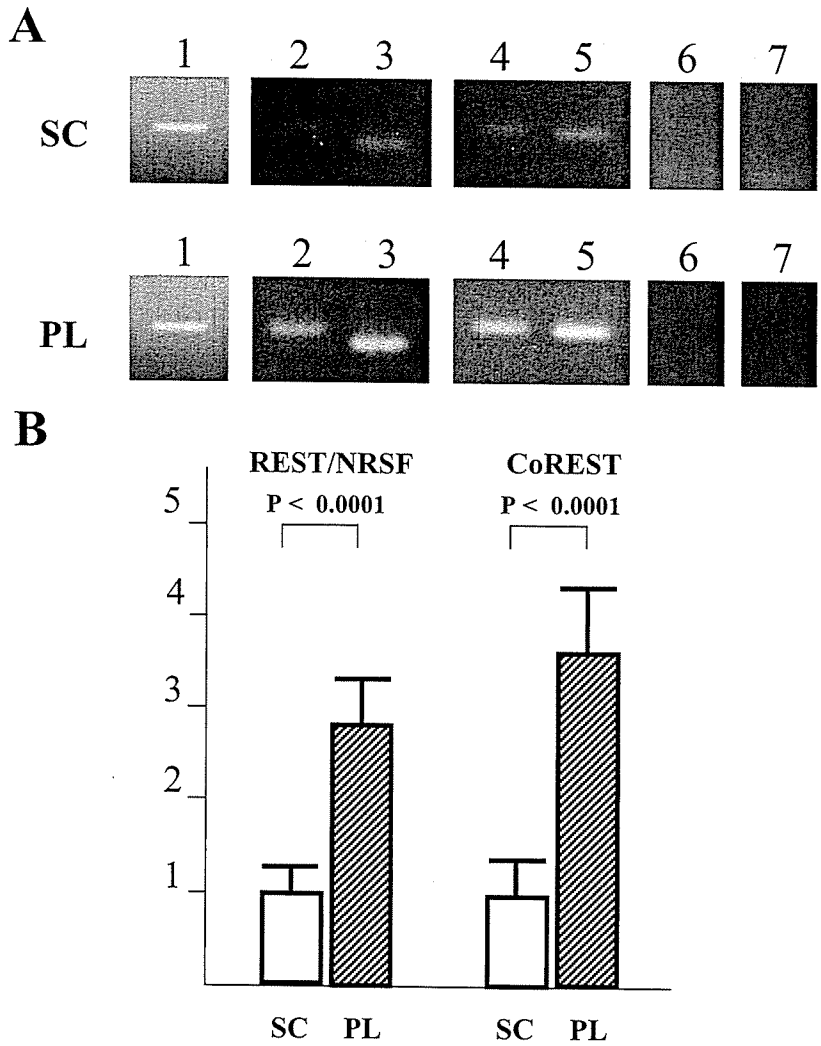

Fig. 5. (A) Agarose-gel electrophoresis of the RT-PCR products of β-actin (lane 1), REST/NRSF (lane 2, with a set of forward primer 1 and reverse primer 1; lane 3, with a set of forward primer 2 and reverse primer 2), and CoREST (lane 4, with a set of forward primer 1 and reverse primer 1; lane 5, with a set of forward primer 2 and reverse primer 2), using RNAs isolated from human spinal cord (SC) and term placenta (PL) tissue homogenates. Lane 6, PCR for REST/NRSF using a set of forward primer 2 and reverse primer 2, without a step of reverse-transcriptase reaction. Lane 7, PCR for CoREST using a set of forward primer 2 and reverse primer 2, without a step of reverse-transcriptase reaction. (B) Relative quantification of REST/NRSF and CoREST transcriptions in the spinal cord (SC) and term placenta (PL).

Detection of REST/NRSF and CoREST mRNAs

REST/NRSF and CoREST mRNAs were detected both in the spinal cord and term placenta by RT-PCR. Direct sequence analysis of the PCR products for REST/NRSF showed that exon N was not included between exons V and VI, either in the spinal cord, or in the placenta, suggesting that REST/NRSF of the spinal cord is identical to that of the placenta. However, the amounts of the REST/NRSF and CoREST RT-PCR products in the placenta were approximately 2.8 and 3.5 times as many as those in the spinal cord, respectively (Fig. 5). Further laser capture microdissection analyses showed that the amounts of PCR products for REST/NRSF and CoREST mRNAs in the placental trophoblastic cells were approximately 2.3 and 2.6 times as many as those in the spinal large motor neurons, respectively (Fig. 6).

Immunohistochemical detection of ChAT and VAChT

Spinal cord. The cytoplasm of the large motor neurons in the anterior horn was diffusely or focally stained with anti-ChAT antibody (Fig. 7A), as already reported (Muroishi et al., 2000). Granular immunoreaction products for VAChT were observed diffusely in the cytoplasm of all large motor neurons (Fig. 7B). VAChT-immunoreactive nerve fibers were scattered throughout the gray and white matter of the spinal cord. Most of the fibers were discontinuously labeled with anti-VAChT antibody.

Placenta. Immunoreaction product deposits for ChAT were evident in the spindle-shaped stromal cells and the endothelial cells of the placental villi (Fig. 7C). Flat trophoblastic cells were occasionally stained with anti-ChAT antibody. There were no immunoreaction

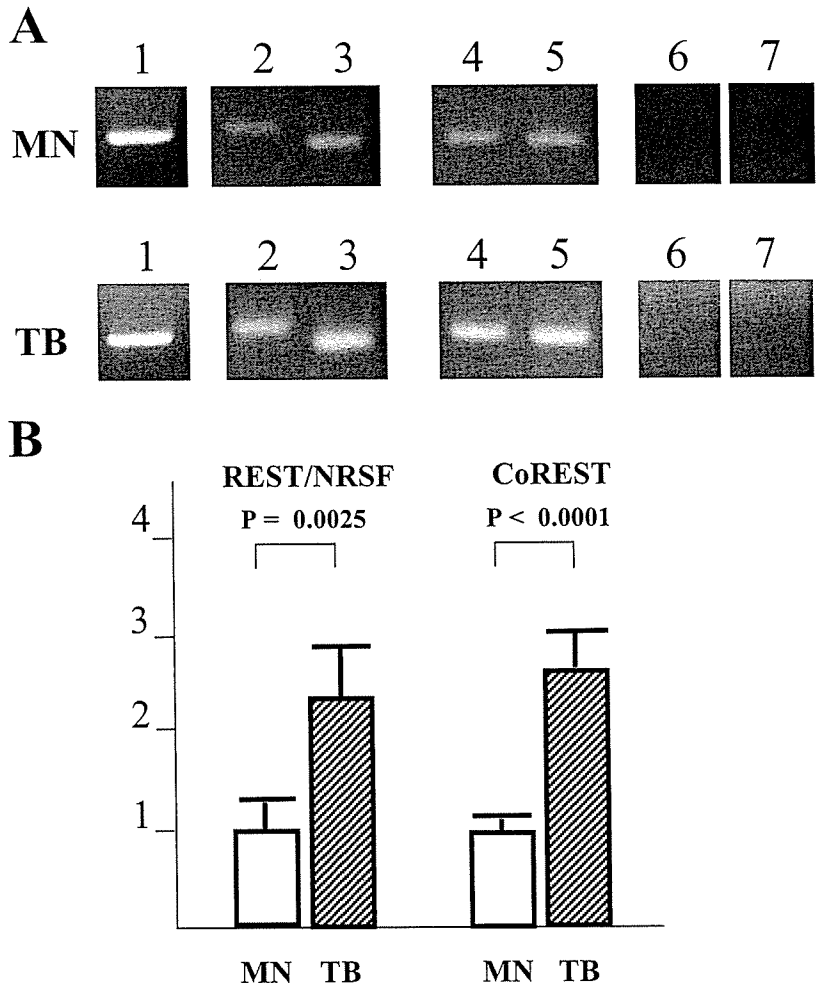

Fig. 6. (A) Agarose-gel electrophoresis of the RT-PCR products of β-actin (lane 1), REST/NRSF (lane 2, with a set of forward primer 1 and reverse primer 1; lane 3, with a set of forward primer 2 and reverse primer 2), and CoREST (lane 4, with a set of forward primer 1 and reverse primer 1; lane 5, with a set of forward primer 2 and reverse primer 2), using RNAs isolated from spinal large motor neurons (MN) and placental trophoblastic cells (TB), obtained by microdissection. Lane 6, PCR for REST/NRSF using a set of forward primer 2 and reverse primer 2 without a step of reverse-transcriptase reaction. Lane 7, PCR for CoREST using a set of forward primer 2 and reverse primer 2 without a step of reverse-transcriptase reaction. (B) Relative quantification of REST/NRSF and CoREST transcriptions in spinal large motor neurons (MN) and placental trophoblastic cells (TB), obtained by microdissection.

products for VAChT in any structures of the placenta (Fig. 7D).

Control experiments in which the primary antibody was replaced by a non-immune rabbit or rat Ig G resulted in no specific cell staining in the spinal cord and placenta tissue sections.

DISCUSSION

In this study, an anti-human VAChT antibody was developed using the C-terminal cytoplasmic domain. The antibody detected a single band of approximately 75 kDa in the crude membrane fractions of the spinal cord. The molecular weight was in good agreement with a report regarding human VAChT expressed in cultured PC-12 cells using the cDNA (Varoqui and Erickson, 1996). The present result not only verifies the specificity of the antibody developed in this study, but also indicated the molecular weight of the native VAChT protein in the human spinal cord. The molecular weight was much greater than the calculated molecular weight of a deduced amino acid sequence from the VAChT DNA (approximately 57 kDa), indicating that the human VAChT is glycosylated, as already speculated (Erickson et al., 1994).

As far as human materials are handled to the experiments, the possibility of degradation of mRNAs is not completely excluded. However, a recent report (Preece et al., 2003) has shown that postmortem human brain mRNA can be used as a quantitatively and statistically ordered study. We examined multiple samples, in which β-actin and β2-microglobulin mRNAs, intrinsic markers, were well preserved. In addition, the postmortem periods in the autopsy cases were relatively short. Therefore, we think that the present study could provide limited but important information on the regulation of the cholinergic gene locus *in vivo*.

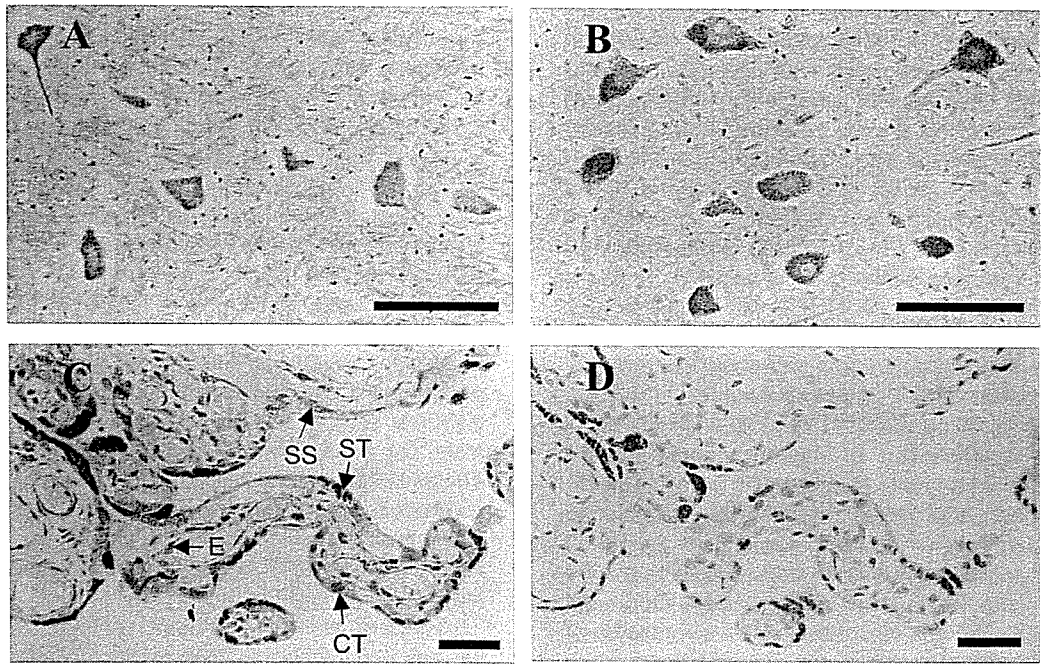

Fig. 7. Immunohistochemistry of ChAT (A and C) and VAChT (B and D) in the human spinal cord (A and B) and term placenta (C and D). CT, cytotrophoblast; E, endothelial cells; SS, spindle-shaped stromal cells; ST, syncytiotrophoblast. Scale bar=100 μm.

Southern blot analysis following RT-PCR showed that the human spinal cord contains the H-type, M-type, N2-type, and R-type ChAT mRNAs. The H-type, N2-type, and R-type mRNAs encode the small form of the ChAT protein with a molecular weight of approximately 68 kDa (Misawa et al., 1997; Robert and Quirin-Stricker, 2001), and the M-type can generate the large (approximately 82 kDa) and the small forms of the ChAT protein (Oda et al., 1992; Misawa et al., 1997; Resendes et al., 1999). The M-type, N2-type, and R-type ChAT mRNAs were isolated from the human spinal cord (Oda et al., 1992; Misawa et al., 1997). The H-type ChAT mRNA was identified at first in the placenta, and not detected in the human spinal cord or human neuroblastoma cell lines (Robert and Quirin-Stricker, 2001). However, the present study showed that the spinal cord tissue from all three autopsied patients contained the H-type ChAT mRNA. In our study, short lengths between exon H and the common coding exon 1 (Robert and Quirin-Stricker, 2001) were targeted to amplify, so that the H-type mRNA could be more easily detected in the autopsied human spinal cord where mRNAs were degraded into small fragments. In addition to ChAT mRNAs, VAChT and CHT1 mRNAs were detected in the spinal cord. Immunohistochemistry showed the VAChT protein in the large motor neurons of the spinal cord. VCAhT-immunoreactive nerve fibers were present not only in the anterior horn, but also in other areas, including the white matter. Most of the immunoreactive nerve fibers were probably derived from cholinergic neurons in other segments of the spinal cord or outside the spinal cord. The present study did not reveal the localization of the CHT1 molecules in the human spinal cord. However, by *in situ* hybridization histochemistry and immunohistochemistry, Kobayashi et al. (2002) and Misawa et al. (2001) have already demonstrated the CHT1 mRNA and the protein in the somatic motor neurons, sympathetic preganglionic neurons, and neurons in the medial part of lamina VII of the human spinal cord. The mRNA for CHT1 is co-localized with the mRNAs for VAChT and ChAT in the somatic motor neurons (Kobayashi et al., 2002).

In contrast, the human term placenta exclusively transcribed the M-type ChAT mRNA. The H-type and N2-type were minor transcripts, and the R-type was not expressed in the term placenta. These results are partly consistent with those by Robert and Quirin-Stricker (2001), showing that the human placenta at 8 months' gestation transcribes the H-type and M-type mRNAs, but not the N- and R-types. It is possible that the H-type and N-type ChAT mRNAs are not abundantly, nor constantly expressed in the term placenta, and therefore, these types of ChAT mRNA might be undetected in some instances.

The present study clearly demonstrated by both RT-PCR and immunohistochemistry that VAChT was not expressed in the human term placenta. The regulatory elements of ChAT and VAChT genes in mammalian cholinergic cells are not fully understood. However, recent *in vitro* expression studies have demonstrated that a 2336-bp rat genomic region upstream from exon R of the ChAT and VAChT exons, which contains a 21-bp sequence homologous to RE1/NRSE, contributes to the neuron-specific expression of ChAT and VAChT (Lönnerberg et al., 1996; De Gois et al., 2000). In non-neuronal cells, the activities of native promoters for both R-type ChAT and VAChT are strongly suppressed by several nuclear proteins binding with this region (De Gois et al., 2000). The 5′-region upstream from exon R in the human cholinergic gene locus is highly homologous to the corresponding rat genomic region, and contains a RE1/NRSE consensus sequence

(Hahm et al., 1997). Therefore, it is reasonable to suppose that transcriptions of both the R-type ChAT and VAChT mRNAs are co-suppressed in the human term placenta by similar mechanisms involving the consensus motif, but those of the M-type and N-type mRNAs, which generate the same enzyme, are independent of the control by RE1/NRSE. This hypothesis is further supported by transgenic mice experiments. Lönnerberg et al. (1995) showed that a rat 2336-bp-long segment from the 5′-flanking region of ChAT exon R directs reporter gene expression (chloramphenicol acetyltransferase) by a heterologous promoter in the ventral spinal cord and brain. On the other hand, Naciff et al. (1997) found a promoter that provides expression of the β-galactosidase reporter gene in the cholinergic neurons of transgenic mice within a 6417-bp DNA fragment between mouse ChAT exons R and M. These studies indicate the presence of at least two separate regulatory elements upstream and downstream of exon R in rodents, both of which control ChAT gene expression.

RE1/NRSE binds to a nuclear factor, REST/NRSF, and represses the transcription of several neuron-specific genes in non-neuronal cells (Schoenherr and Anderson, 1995a; Schoenherr et al., 1996). REST/NRSF is known to further interact with other co-repressors, such as mSin3 and CoREST, and recruits histone deacetylase to form a complex. The complex is believed to change chromatin conformation near RE1/NRSE, causing the expression of RE1/NRSE-containing genes in non-neuronal cells to be repressed (Jones and Meech, 1999). However, diverse results have been reported as to the expression of REST/NRSF in cultured nerve cells or the neuronal tissues of laboratory animals; some neuronal cell lines express REST/NRSF (Chong et al., 1995: Bessis et al., 1997), but some others do not (De Gois et al., 2000). A developmental study of the mouse embryo detected REST/NRSF mRNA in undifferentiated neuronal progenitors, but not in differentiated neurons (Schoenherr and Anderson, 1995b). On the other hand, primary cultures of newborn rat dorsal root ganglion neurons expressed REST/NRSF (Chong et al., 1995). These results suggest that expression depends on cell lines, conditions, or developmental stages. Up to now, the expressions of REST/NRSF and CoREST have not been recognized in human nervous tissue *in vivo*.

In the present study, we examined whether the different transcriptional regulation of the R-type ChAT and VAChT between the human spinal cord and placenta is related to the presence or absence of REST/NRSF and CoREST in the tissues. REST/NRSF and CoREST were transcribed in the spinal cord and term placenta. Neuron-specific REST/NRSF transcripts, which contain a 4- (hREST N4) or a 62-bp (hREST N62) insertion between exons V and VI and encode truncated REST protein isoforms with low DNA-binding activity (Palm et al., 1999), were not detected in the spinal cord. However, the amounts of the REST/NRSF and CoREST mRNAs were higher in the placenta than in the spinal cord. Further comparative analyses using a microdissection technique were added to investigate whether these regulatory molecules are expressed differently in the spinal motor neurons and placental trophoblastic cells, revealing that there were more REST/NRSF and CoREST mRNAs in the placental trophoblastic cells than in the spinal large motor neurons. These results are consistent in part with the experimental studies of REST/NRSF expression using adult rat brains (Palm et al., 1998), rat dorsal root ganglion neurons (Chong et al., 1995), and cultured cell lines (Chong et al., 1995; Bessis et al., 1997), which showed that REST/NRSF is also expressed in mature neurons, but the transcription level is relatively low in neurons compared with non-neuronal cells. Chong et al. (1995) suggested that the effect of REST/NRSF is graded and high expression levels of REST/NRSF are necessary to silence neuron-specific genes in non-neuronal cells. Thus, taken together with these experimental studies and the present results, it is suggested that transcription of R-type ChAT and VAChT is suppressed in the term placenta with high transcription levels of REST/NRSF and CoREST, but not in the spinal cord with low transcription levels of both molecules. However, REST/NRSF silencing is likely to be promoter specific. The specificity may be determined by the particular combination of regulatory factors, some of which have not been identified yet (Jones and Meech, 1999). Therefore, the control mechanism for the expression of the cholinergic gene locus involving RE1/NRSE may function with a combination of other regulatory elements with REST/NRSF and CoREST in the human term placenta. Further studies are required to resolve the issue.

In conclusion, the present study showed that gene expression of the molecules responsible for ACh metabolism is different between the human spinal cord and term placenta. It is suggested that at least two separate regulatory mechanisms of gene expression are present for the human cholinergic gene locus, which are possibly selected by different combinations of DNA motifs and binding proteins to function in neuronal and non-neuronal cells.

Acknowledgments—This research was supported by grants from the Ministry of Education, Science and Culture of Japan (to Y. Oda).

REFERENCES

Apparsundaram S, Ferguson SM, George AL Jr, Blakely RD (2000) Molecular cloning of a human, hemicholinium-3-sensitive choline transporter. Biochem Biophys Res Commun 276:862–867.

Benjanin S, Cervini R, Mallet J, Berrard S (1994) A unique gene organization for two cholinergic markers, choline acetyltransferase and a putative vesicular transporter of acetylcholine. J Biol Chem 269:21944–21947.

Berrard S, Varoqui H, Cervini R, Israël M, Mallet J, Dieber M-F (1995) Coregulation of two embedded gene products, choline acetyltransferase and the vesicular acetylcholine transporter. J Neurobiol 65:939–942.

Berse B, Blusztajn JK (1995) Coordinated up-regulation of choline acetyltransferase and vesicular acetylcholine transporter gene expression by the retinoic acid receptor a, cAMP, and leukemia inhibitory factor/ciliary neurotrophic factor signaling pathways in a murine septal cell line. J Biol Chem 270:22101–22104.

Bessis A, Champtiaux N, Chatelin L, Changeux J-P (1997) The neuron-restrictive silencer element: a dual enhancer/silencer crucial for patterned expression of a nicotinic receptor gene in the brain. Proc Natl Acad Sci USA 94:5906–5911.

Cervini R, Houhou L, Pradat P-F, Béjanin S, Mallet J, Berrard S (1995) Specific vesicular acetylcholine transporter promoters lie within the

first intron of the rat choline acetyltransferase gene. J Biol Chem 270:24654–24657.
Chong JA, Tapia-Ramírez J, Kim S, Toledo-Arai JJ, Zheng Y, Boutros MC, Altshuller YM, Frohman MA, Kraner SD, Mandel G (1995) REST: a mammalian silencer protein that restricts sodium channel gene expression to neurons. Cell 80:949–957.
De Gois S, Houhou L, Oda Y, Corbex M, Pajak F, Thévenot E, Vodjdani G, Mallet J, Berrard S (2000) Is RE1/NRSE a common cis-regulatory sequence for ChAT and VAChT genes? J Biol Chem 275:36683–36690.
Erickson JD, Varoqui H, Schäfer MK-H, Modi W, Diebler M-F, Weihe E, Rand J, Eiden LE, Bonner TI, Usdin TB (1994) Functional identification of a vesicular acetylcholine transporter and its expression from a 'cholinergic' gene locus. J Biol Chem 269:21929–21932.
Hahm SH, Chen L, Patel C, Erickson J, Bonner TI, Weihe E, Schäfer MK-H, Eiden LE (1997) Upstream sequencing and functional characterization of the human cholinergic gene focus. J Mol Neurosci 9:223–236.
Jones FS, Meech R (1999) Knockout of REST/NRSF shows that the protein is a potent repressor of neuronally expressed genes in non-neural tissues. Bioessays 21:372–376.
King RG, Gude NM, Krishna BR, Chen S, Brenncke SP, Boura ALA, Rook TJ (1991) Human placental acetylcholine. Reprod Fertil Dev 3:405–411.
Kobayashi Y, Okuda T, Fujioka Y, Matsumura G, Nishimura Y, Haga T (2002) Distribution of the high-affinity choline transporter in the human and macaque monkey spinal cord. Neurosci Lett 317:25–28.
Lönnerberg P, Lendahl U, Funakoshi H, Arhlund-Richter L, Persson H, Ibáñez CF (1995) Regulatory region in choline acetyltransferase gene directs developmental and tissue-specific expression in transgenic mice. Proc Natl Acad Sci USA 92:4046–4050.
Lönnerberg P, Schoenherr CJ, Anderson DJ, Ibáñez CF (1996) Cell type-specific regulation of choline acetyltransferase gene expression. J Biol Chem 273:33358–33365.
Misawa H, Matsuura J, Oda Y, Takahashi R, Deguchi T (1997) Human choline acetyltransferase mRNAs with different 5′-region produce a 69-kDa major translation product. Mol Brain Res 44:323–333.
Misawa H, Nakata K, Matsuura J, Nagao M, Okuda T, Haga T (2001) Distribution of the high-affinity choline transporter in the central nervous system of the rat. Neuroscience 105:87–98.
Misawa H, Takahashi R, Deguchi T (1995) Coordinate expression of vesicular acetylcholine transporter and choline acetyltransferase in sympathetic superior cervical neurons. Neuroreport 6:965–968.
Muroishi Y, Kasashima S, Nakanishi I, Oda Y (2000) Immunohistochemical and in situ hybridization studies of choline acetyltransferase in large motor neurons of the human spinal cord. Histol Histopathol 15:689–696.
Naciff JM, Misawa H, Dedman JR (1997) Molecular characterization of the mouse vesicular acetylcholine transporter. Neuroreport 8:3467–3473.
Noonan KE, Beck C, Holzmayer TA, Chin JE, Wunder JS, Andrulis IL, Gazdar AF, Willman CL, Griffith B, Von Hoff DD, Roninson IB (1990) Quantitative analysis of MDR1 (multidrug resistance) gene expression in human tumors by polymerase chain reaction. Proc Natl Acad Sci USA 87:7160–7164.
Oda Y (1999) Choline acetyltransferase: the structure, distribution and pathologic changes in the central nervous system. Pathol Int 49:921–937.
Oda Y, Imai S, Nakanishi I, Ichikawa T, Deguchi T (1995) Immunohistochemical study on choline acetyltransferase in the spinal cord of patients with amyotrophic lateral sclerosis. Pathol Int 45:933–939.
Oda Y, Nakanishi I, Deguchi T (1992) A complementary DNA for human choline acetyltransferase induces two forms of enzyme with different molecular weights in cultured cells. Mol Brain Res 16:287–294.
Oda Y, Yamashita N, Muroishi Y, Nakanishi I (1996) Localization of choline acetyltransferase and acetylcholine in the chorion of early human placenta. Histochem Cell Biol 105:93–99.
Okuda T, Haga T (2000) Functional characterization of the human high-affinity choline transporter. FEBS Lett 484:92–97.
Okuda T, Haga T, Kanai Y, Endou H, Ishihara T, Katsura I (2000) Identification and characterization of the high-affinity choline transporter. Nat Neurosci 3:120–125.
Palm K, Belluardo N, Metsis M, Timmusk T (1998) Neuronal expression of zinc finger transcription factor REST/NRSF/XBR gene. J Neurosci 18:1280–1296.
Palm K, Metsis M, Timmusk T (1999) Neuron-specific splicing of zinc finger transcription factor REST/NESF/XBR is frequent in neuroblastomas and conserved in human, mouse and rat. Mol Brain Res 72:30–39.
Preece P, Virley DJ, Costandi M, Coombes R, Moss SJ, Mudge AW, Jazin E, Cairns NJ (2003) An optimistic view for quantifying mRNA in post-mortem human brain. Mol Brain Res 116:7–16.
Resendes MC, Dobransky T, Ferguson SSG, Rylett RJ (1999) Nuclear localization of the 82-kDa form of human choline acetyltransferase. J Biol Chem 274:19417–19421.
Robert I, Quirin-Stricker C (2001) A novel untranslated 'exon H' of the human choline acetyltransferase gene in placenta. J Neurochem 79:9–16.
Roghani A, Feldman J, Kohan SA, Shirzadi A, Gundersen CB, Brecha N, Edwards RH (1994) Molecular cloning of a putative vesicular transporter for acetylcholine. Proc Natl Acad Sci USA 91:10620–10624.
Roghani A, Shirzadi A, Butcher LL, Edwards RH (1998) Distribution of the vesicular transporter for acetylcholine in the rat central nervous system. Neuroscience 82:1195–1212.
Sambrook J, Fritsch EF, Maniatis T (1989) Molecular cloning: a laboratory manual. 2nd ed. New York: Cold Spring Harbor Laboratory.
Sastry BVR (1997) Human placental cholinergic system. Biochem Pharmacol 53:1577–1586.
Sastry BVR, Sadavongvivad C (1979) Cholinergic systems in non-nervous tissues. Pharmacol Rev 30:65–132.
Schoenherr CJ, Anderson DJ (1995a) Silencing is golden: negative regulation in the control of neuronal gene transcription. Curr Opin Neurobiol 5:566–571.
Schoenherr CJ, Anderson DJ (1995b) The neuron-restrictive silencer factor (NRSF): a coordinate repressor of multiple neuron-specific genes. Science 267:1360–1363.
Schoenherr CJ, Paquette AJ, Anderson DJ (1996) Identification of potential target genes for the neuron-restrictive silencer factor. Proc Natl Acad Sci USA 93:9881–9886.
Stabile I, Teaf CM, Harbison RD (1989) Role of cholinergic and carnitinergic systems in placental toxicology. Contemp Rev Obstet Gynecol 1:253–260.
Tanaka H, Zhao Y, Wu D, Hersh LB (1998) The use of Dnase I hypersensitivity site mapping to identify regulatory regions of the human cholinergic gene locus. J Neurochem 70:1799–1808.
Varoqui H, Erickson J (1996) Active transport of acetylcholine by the human vesicular acetylcholine transporter. J Biol Chem 271:27229–27232.
Voller A, Bidwell DE, Bartlett A (1976) Enzyme immunoassays in diagnostic medicine, therapy and practice. Bull WHO 53:55–64.
Wessler I, Kirkpatrick CJ, Racké K (1998) Non-neuronal acetylcholine, a locally acting molecule, widely distributed in biological systems: expression and function in humans. Pharmacol Ther 77:59–79.

(Accepted 1 June 2004)
(Available online 10 August 2004)

European Journal of Neuroscience, Vol. 20, pp. 353–362, 2004

c-ret regulates cholinergic properties in mouse sympathetic neurons: evidence from mutant mice

K. Burau,[1] I. Stenull,[1] K. Huber,[1] H. Misawa,[2] B. Berse,[3] K. Unsicker[1] and U. Ernsberger[1]
[1]Interdisciplinary Center for Neurosciences, Department of Neuroanatomy, University of Heidelberg, INF 307, D-69120 Heidelberg, Germany
[2]Tokyo Metropolitan Institute for Neuroscience, Department of Neurology, Fuchu City, Japan
[3]Boston University School of Medicine, Department of Pathology and Laboratory Medicine, Boston, MA, USA

Keywords: choline acetyltransferase, development, ret, vesicular acetylcholine transporter

Abstract

The search for signalling systems regulating development of noradrenergic and cholinergic sympathetic neurons is a classical problem of developmental neuroscience. While an essential role of bone morphogenetic proteins for induction of noradrenergic properties is firmly established, factors involved in the development of cholinergic traits *in vivo* are still enigmatic. Previous studies have shown that the c-ret receptor and cholinergic properties are coexpressed in chick sympathetic neurons. Using *in situ* hybridization we show now that a loss-of-function mutation of the c-ret receptor in mice dramatically reduces numbers of cells positive for choline acetyltransferase (ChAT) and the vesicular acetylcholine transporter (VAChT) in stellate ganglia of homozygous newborn animals. The number of neurons positive for tyrosine hydroxylase (TH) mRNA, the rate-limiting enzyme of noradrenaline synthesis, is reduced to a smaller degree and expression levels are not detectably altered. Already at embryonic day 16 (E16), ChAT and VAChT-positive cells are affected by the c-ret mutation. At E14, however, ChAT and VAChT mRNAs are detectable at low levels and no difference is observed between wildtype and mutant mice. Our data suggest that c-ret signalling is necessary for the maturation of cholinergic sympathetic neurons but dispensable for *de novo* induction of ChAT and VAChT expression.

Introduction

The development of the transmitter phenotype in sympathetic neurons is a classical model for studying the molecular basis of neuronal differentiation (reviewed in Ernsberger, 2001). Different populations of sympathetic neurons employ noradrenaline or acetylcholine, respectively, for synaptic transmission and can be distinguished by expression of the respective transmitter-synthesizing enzymes (reviewed in Ernsberger & Rohrer, 1999). While there is general consensus that bone morphogenetic proteins (BMPs) at the dorsal aorta are necessary for induction of the noradrenergic transmitter phenotype (reviewed in Ernsberger, 2000; Goridis & Rohrer, 2002), the molecular bases of induction of cholinergic properties is incompletely understood. Whereas sympathetic sweat gland innervation in rodents develops cholinergic properties in response to target-derived signals (reviewed in Landis, 1990; Schotzinger *et al.*, 1994), other sympathetic neuron populations become cholinergic before target innervation (reviewed in Ernsberger & Rohrer, 1999).

Studies in chick embryos have indicated that early and late embryonic expression of cholinergic properties in sympathetic neurons may be regulated via different signalling systems. gp130 and the leukaemia inhibitory factor receptor β (LIFRβ), components of the neurokine receptor complex, are involved in the late, possibly target-dependent maturation of cholinergic sympathetic neurons (Geissen *et al.*, 1998; Duong *et al.*, 2002). Suppression of gp130 or LIFRβ expression by retrovirally mediated antisense RNA interferes with expression of vasoactive intestinal polypeptide (VIP), a widely used marker of cholinergic neurons, without altering expression of the enzyme for acetylcholine biosynthesis, choline acetyltransferase (ChAT), and the vesicular acetylcholine transporter (VAChT). This suggests that different features of cholinergic properties may be distinctly regulated *in vivo*. *In vitro*, the neurokine ciliary neurotrophic factor (CNTF) affects ChAT expression at advanced but not at young developmental stages (Ernsberger *et al.*, 1997). In addition to neurokines, members of the glial cell line-derived growth factor family (GFL) and the neurotrophin family were shown to promote cholinergic properties *in vitro* (Brodski *et al.*, 2000, 2002).

c-ret, a receptor tyrosine kinase involved in GFL signal transduction (Airaksinen & Saarma, 2002), is coexpressed with cholinergic markers in chick sympathetic neurons (Ernsberger *et al.*, 2000; Brodski *et al.*, 2002). The onset of c-ret expression prior to cholinergic differentiation (Robertson & Mason, 1995; Ernsberger *et al.*, 1997) had suggested that signalling via c-ret may be involved in the development of the cholinergic transmitter phenotype in sympathetic neurons *in vivo*. In the present study, mice with a mutation in the kinase domain of c-ret (Schuchardt *et al.*, 1994) were analysed to provide evidence that c-ret signalling is involved in the development of cholinergic sympathetic neurons. Expression levels of ChAT or VAChT mRNA are strongly reduced in sympathetic stellate ganglia of homozygous mutant mice at the time of birth, but unaffected at embryonic days 13 and 14. Our results suggest that initial induction of cholinergic properties occurs independent of c-ret activity. For expression of normal levels of ChAT and VAChT mRNAs at later stages, however, c-ret activity is indispensable. Preliminary parts of these data have been presented in abstract form (Burau *et al.*, 2002).

Correspondence: Dr U. Ernsberger, as above.
E-mail: uwe.ernsberger@urz.uni-heidelberg.de

Received 22 December 2003, revised 4 May 2004, accepted 11 May 2004

doi:10.1111/j.1460-9568.2004.03500.x

Materials and methods

Animals

Mice with a targeted mutation of the gene coding for c-ret consisting of a truncation of the intracellular tyrosine kinase domain (Schuchardt *et al.*, 1994) were bred in a C57Bl6 background. Genotyping was performed with PCR on genomic DNA as described by Allmendinger *et al.* (2003) and supported by analysis of kidney development as well as analysis of c-ret mRNA expression by *in situ* hybridization.

Animals are kept at the Central Animal Facility (ZTL) of the Heidelberg University according to the Regulations for Animal Welfare (Tierschutzgesetz).

Tissue preparation

Offspring was collected immediately after birth or at embryonic days 13 (E13), 14 (E14), and 16 (E16). The time when the vaginal plug was detected was counted as day 0. Pregnant females were killed by CO_2 asphyxiation. Newborn animals were kept on ice prior to transcardial perfusion with 4% paraformaldehyde and postfixed in 4% paraformaldehyde overnight. Embryos were fixed by immersion in 4% paraformaldehyde overnight. After fixation, animals were dehydrated by treatment with 15% sucrose overnight and cryosectioned after embedding in Tissue Tec (Sakura, Zoeterwoude, Netherlands). Cross sections from the neck and upper thoracic regions were taken at 12 μm thickness, dried at 37 °C for 1 h and stored at −20 °C.

In situ *hybridization (ISH)*

TH and dopamine β-hydroxylase (DBH) riboprobes (generously provided by Drs C. Goridis and J.F. Brunet, Ecole Normale Supérieure, Paris, France) were used for ganglion localization and detection of noradrenergic properties as described (Huber *et al.*, 2002). Riboprobes for mouse ChAT (Ishii *et al.*, 1990) and VAChT (741b; position 1124–1864, GenBank accession number AF019045) were used to analyse expression from the cholinergic gene locus. *In situ* hybridization was performed as described by Ernsberger *et al.* (1997, 2000). Specificity of the reaction product in ChAT and VAChT ISH was confirmed with corresponding sense riboprobes.

Histological analysis

At E16 and P0, ISH signals were sufficiently strong to allow quantitative analysis of positive cells. At E13 and E14, ChAT and VAChT ISH signals were distinctly above background but too low to count positive cells.

To quantitatively assess ganglion size and cell number in newborn and E16 animals, cross sections of the neck region were taken at 12 μm thickness and ganglion area was determined after TH or DBH *in situ* hybridization from every tenth section. The rostral end of the ganglion could be easily identified. Due to different degrees of fusion with thoracic ganglia, the caudal end of the stellate ganglion was defined as the section with the first ganglionic area minimum showing less than 50% of the largest extension of the ganglion. Ganglion volume was derived from the rostrocaudal extension and the area measurements. To estimate the number of ganglionic cells, somata with large round to oval nucleus were counted on 12-μm cross-sections hybridized for TH, VAChT or ChAT, and controlled by DAPI staining. These numbers are shown as cell counts per area. To derive ganglionic cell numbers, cell counts are transformed to counts per volume and corrected according to the Linderstrom-Lang/Abercrombie equation (Hedreen, 1998).

To estimate numbers of ChAT and VAChT-positive cells in newborn stellate ganglia, the number of positive cells and ganglionic area were determined from every tenth section. To estimate numbers of positive cells in ganglia of E16 animals, the number of sections analysed was increased 2–4-fold to compensate for smaller cell numbers. The density of ChAT and VAChT-positive cells was determined from the counts of positive cells and the area measurements. To derive ganglionic cell numbers, cell counts are transformed to counts per volume and corrected according to the Linderstrom-Lang/Abercrombie equation (Hedreen, 1998).

Statistical analysis

The significance of differences between cell counts was determined with ANOVA (Origin 6.1 software, OriginLab, Northampton, MA, USA) and the Mann–Whitney test (Byrkit, 1987)

Results

Position, size, and cell numbers of stellate ganglia in newborn c-ret mutant mice

As mutation of c-ret may affect the localization of sympathetic ganglia (Enomoto *et al.*, 2001), we first analysed the distribution of sympathetic neurons in the cervical and thoracic region, in particular the stellate ganglia, of wildtype and c-ret mutant mice. For the localization of sympathetic neurons, ISH for TH or DBH mRNAs was performed. In all wildtype animals and heterozygous mutants, large nerve cell aggregates were well aligned with the thymus (Fig. 1). The rostral start of these ganglionic structures was clearly defined, whereas the caudal end was less distinctly recognizable due to different degrees of fusion with more caudally located nerve cell clusters. In homozygous mutants, the situation was the same in two out of three animals. In one animal, the large nerve cell clusters were markedly displaced along the rostrocaudal axis such that ganglionic structures came to lie rostrally and caudally to the thymus (Fig. 1, animal 2.8). This corroborates and extends previous observations concerning discrete alterations in the position of sympathetic ganglia, especially the superior cervical ganglia, in c-ret and GFL alpha-receptor knockout mice (Nishino *et al.*, 1999; Enomoto *et al.*, 2001).

Sympathetic ganglion size including stellate ganglion size was reported to be reduced in ret mutants (Enomoto *et al.*, 2001). Due to the various degrees of fusion of stellate and thoracic ganglia already in wildtype animals, this is difficult to quantify. To attempt an estimate of ganglion size and cell number, we defined the stellate ganglion to extend from the easily recognizable cranial end to the first area minimum showing less than 50% of the largest extension of the ganglion. The volume of this ganglionic region was reduced by approximately 50% in homozygous ret mutants as compared to wildtype animals (Table 1). Due to the smaller size of cells in mutant ganglia, as also reported for the SCG of ret mutant animals (Enomoto *et al.*, 2001), and the denser packing in mutant ganglia, the decrease in the estimated ganglionic cell number amounts to 24% (Table 1). Already in heterozygous mutants, similar alterations in ganglion volume, cell density, and estimated cell number were observed (Table 1).

Expression of noradrenergic and cholinergic transmitter phenotypes in stellate ganglia and spinal cord of newborn c-ret mutant mice

Cross sections of the neck region were analysed for noradrenergic and cholinergic differentiation by ISH. mRNAs for TH (Figs 2 and

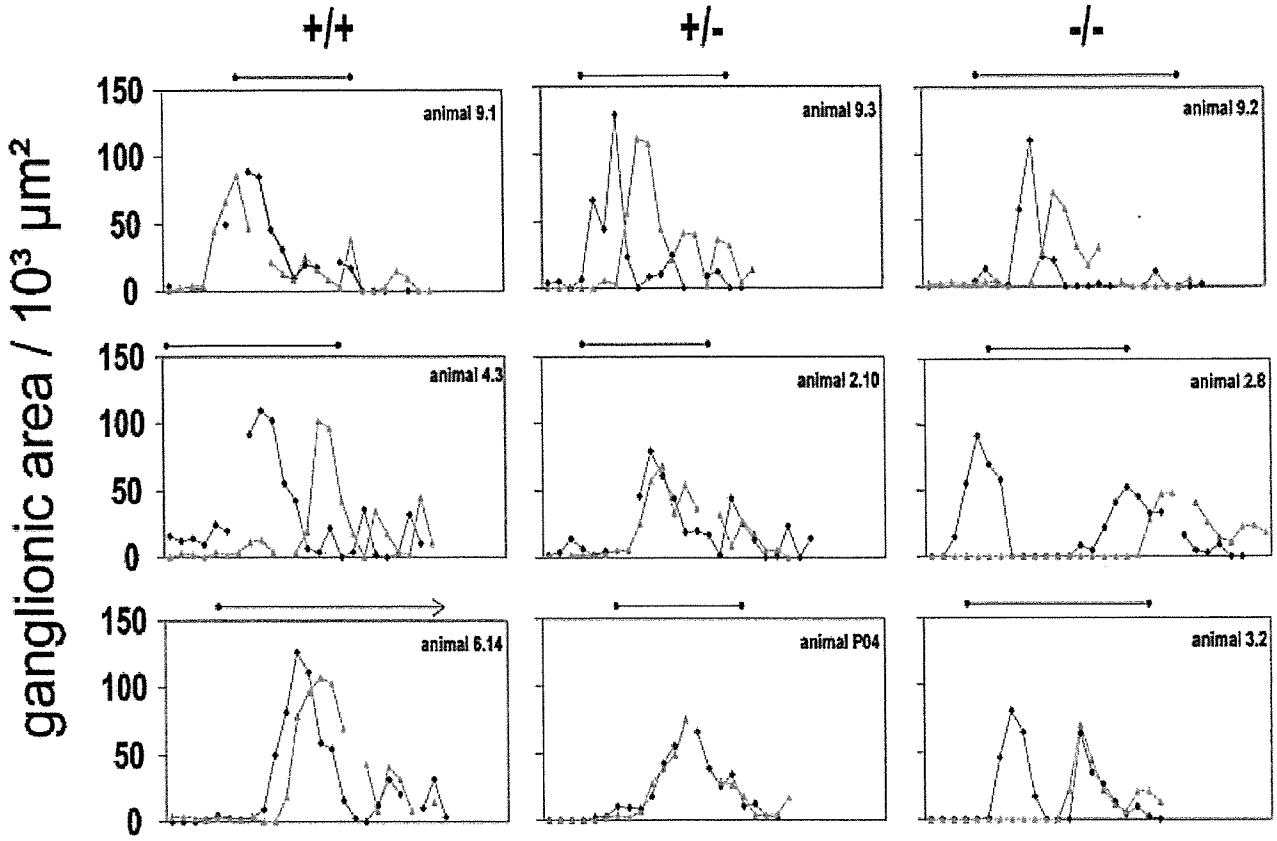

FIG. 1. Position of stellate ganglia in newborn wildtype and c-ret mutant mice. Serial sections in the cervical and thoracic region of wildtype (+/+), heterozygous (+/–), and homozygous (–/–) c-ret mutant mice were hybridized with TH and DBH riboprobes to detect sympathetic ganglion neurons. Ganglion size was determined for the right (black) and left (grey) side independently. Each data point represents the area covered by TH or DBH expressing cells in one section. Adjacent data points are 120 µm apart. Rostral is to the left, caudal to the right. The position of the thymus is indicated by the bar above the plot for each individual animal. The rostral end of the sympathetic neuron aggregates, forming the stellate ganglia, are sharply demarcated. The caudal end is not unequivocally defined due to various degrees of fusion with more caudally located nerve cell clusters. The ganglion position on the right and left side is not always in register. In homozygous c-ret mutants, ganglion position appears normal in two out of three mice. In one animal (2.8), ganglia on both sides are displaced towards the rostral and caudal ends of the thymus. In two homozygous mutants (2.8 and 3.2), two main ganglionic aggregates appear on the right side at the level of the thymus.

TABLE 1. Reduction of stellate ganglion size and cell number in newborn animals

Genotype	Ganglion volume (mm^3)	Cell density (per mm^2)	Cell number estimate (per ganglion)
+/+	0.052 ± 0.0052	4530 ± 339	10375 ± 720
+/–	0.030 ± 0.0027**	5897 ± 132*	7847 ± 772*
–/–	0.026 ± 0.0024**	6369 ± 438*	7936 ± 473*

Ganglion volume and cell density were determined as described in Materials and methods. The cell numbers per ganglion were estimated by transforming the density per area into density per volume and correction by the Linderstrom-Lang/Abercrombie equation (Hedreen, 1998). Mean cell diameters used for correction were obtained from at least 60 cells per genotype: 10.4 µm, wildtype; 10.9 µm, heterozygous; 9.0 µm, homozygous mutants. Values given in the table are means ± SEM from six ganglia each in wildtype and heterozygous mutants and from five ganglia in homozygous mutants. Mutant animals are significantly different from wildtype: $*P < 0.05$, $**P < 0.005$ (ANOVA).

3) and DBH (not shown), enzymes of the noradrenaline biosynthesis cascade, are expressed in stellate ganglia of homozygous c-ret mutant animals supporting the notion that noradrenergic neurons differentiate in spite of the lack of c-ret signalling (Durbec *et al.*, 1996; Enomoto *et al.*, 2001). Choline acetyltransferase (ChAT), the enzyme of acetylcholine biosynthesis, and the vesicular acetylcholine transporter (VAChT) could be detected in spinal cord motor neurons of homozygous c-ret mutants (Fig. 2B and C). In stellate ganglia of homozygous animals, however, expression of the cholinergic markers was drastically reduced, while heterozygous animals showed apparently normal cholinergic cells (Figs 2B–D, and 3A–D).

The relative loss of ChAT and VAChT-positive cells largely exceeds that of total stellate ganglion cells in homozygous c-ret mutant mice

In Fig. 4 the distribution and numbers of ChAT and VAChT mRNA expressing cells are plotted for serial sections through stellate ganglia of wildtype, heterozygous, and homozygous mutant mice. While wildtype and heterozygous stellate ganglia displayed cells positive for ChAT and VAChT mRNAs in almost every section, only very few sections from homozygous mutants contained cholinergic cells. Figure 5 presents numbers of ChAT and

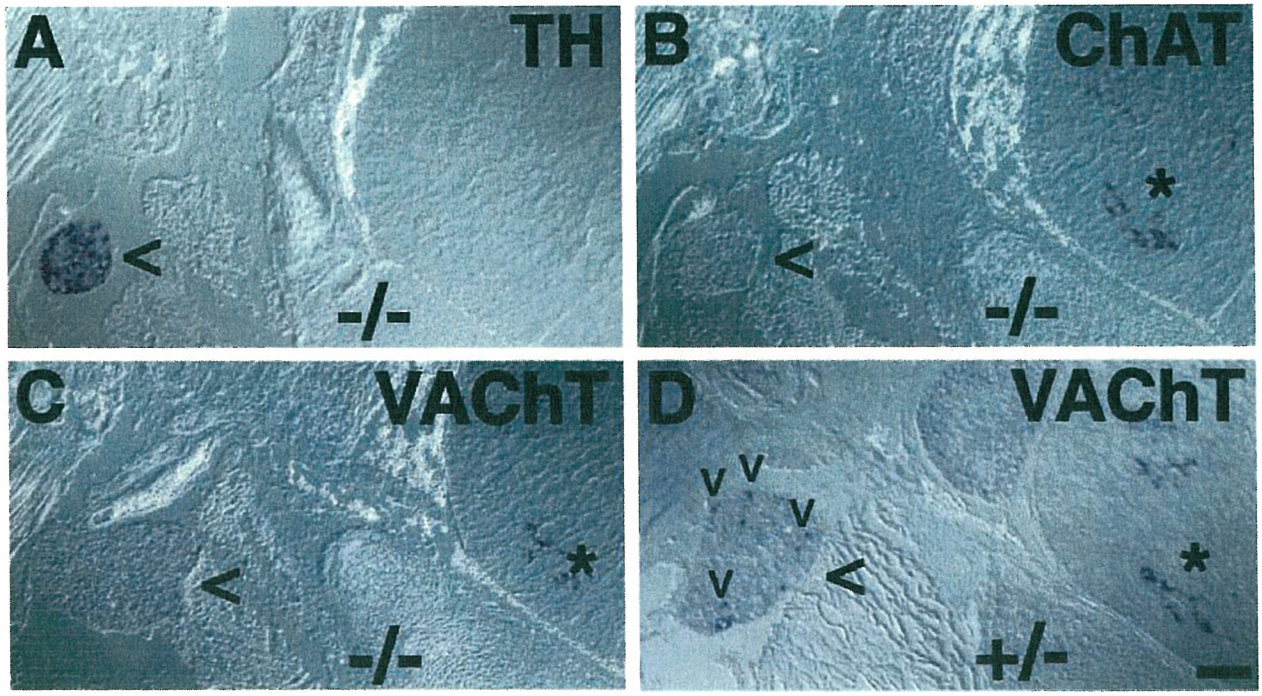

FIG. 2. Expression of noradrenergic and cholinergic properties in sympathetic ganglia and spinal cord of c-ret mutant mice. Sections from heterozygous (+/–) and homozygous (–/–) c-ret mutant mice were hybridized with riboprobes for tyrosine hydroxylase (TH), choline acetyltransferase (ChAT), and the vesicular acetylcholine transporter (VAChT). TH expression is detectable in sympathetic ganglia (<) of homozygous c-ret mutants (A). ChAT (B) and VAChT (C and D) are detected in spinal motoneurons (*) of homozygous (B and C) and heterozygous (D) mutant animals. In sympathetic ganglia (<) of heterozygous animals (D), VAChT expressing cells (v) are detectable whereas no ChAT or VAChT expression is found in sympathetic ganglia (<) of homozygous mutants (B and C). Scale bar, 120 μm.

VAChT-positive cells (identified by ISH) per mm^2 for wildtype, heterozygous, and homozygous c-ret mutant mice. Overall, the density of cells positive for these cholinergic markers is decreased by more than 80% in homozygous mutants as compared to wildtype littermates. No reduction is observed in heterozygous animals.

The absolute number of ChAT-positive cells per stellate ganglion is estimated to be 63.1 ± 12.1 in wildtype and 1.3 ± 1.3 in homozygous mutants, corresponding to a highly significant decrease by 98% ($n \geq 5$ ganglia per genotype; ± SEM; $P = 0.001$, ANOVA). The number of VAChT-positive cells is estimated to be 117.9 ± 22.4 in wildtype animals as compared to 8.8 ± 3.8 in homozygous mutants ($n \geq 5$ ganglia per genotype; ± SEM; $P = 0.002$, ANOVA), corresponding to a highly significant decrease by 93%.

Taken together, the data show a reduction by 24% in total ganglionic cell number and by more than 90% in ChAT and VAChT-positive stellate cells in homozygous c-ret mutant mice. This massive reduction in cells expressing cholinergic markers is due to the combination of reduced ganglionic cell number and a much stronger reduction in the density of cells with detectable ChAT and VAChT mRNA levels. The reduction in density may result from the loss of cells with cholinergic properties or from the lack of detectable expression of cholinergic markers in still existing cells. As numbers of stellate cells expressing ChAT and VAChT mRNAs are small, comparison with total ganglion cell estimates does not allow a decision to be made between the two possibilities. Heterozygous mutation, though sufficient to reduce ganglionic cell numbers, does neither result in reduced densities of ChAT and VAChT-positive cells nor in reduced staining intensities as judged by *in situ* hybridization.

c-ret mutation does not affect TH mRNA expression levels in mouse stellate ganglia

To investigate whether the reduction in cholinergic markers seen in c-ret homozygous mutant mice was transmitter-specific or paralleled by a similar decrease in noradrenergic marker expression, we analysed TH mRNA by ISH. Figure 3E and F shows that TH mRNA positive cells occurred at several distinct levels of staining intensities. Consequently, Fig. 6 presents percentages of TH mRNA positive cells classified according to four distinct levels of mRNA expression (–, +, ++ and +++) by two independent observers. No significant alterations were observed for any of these four categories in c-ret mutant mice. Consequently, the proportion of TH-positive cells including all cells with detectable TH ISH signal (+, ++ and +++) is not altered significantly. They amount to 94.0 ± 2.1% of ganglionic cells in wildtype animals and to 95.7 ± 0.3% in homozygous mutants ($n = 3$ animals, ± SEM). These data demonstrate that the vast majority of ganglionic cells are catecholaminergic cells. Thus, the overall decrease in cell number in c-ret mutants by approximately 25% affects the noradrenergic cell population albeit, relative to population size, to a much smaller degree than >90% reduction of ChAT and VAChT-positive cells in homozygous c-ret mutants.

Expression of cholinergic properties in stellate ganglia is affected already in 16-day-old c-ret mutant animals

In order to establish whether the above changes in cholinergic marker expression of stellate neurons were associated with ontogenetic maturation or initial induction of the cholinergic phenotype, we studied E16 and earlier stellate ganglia.

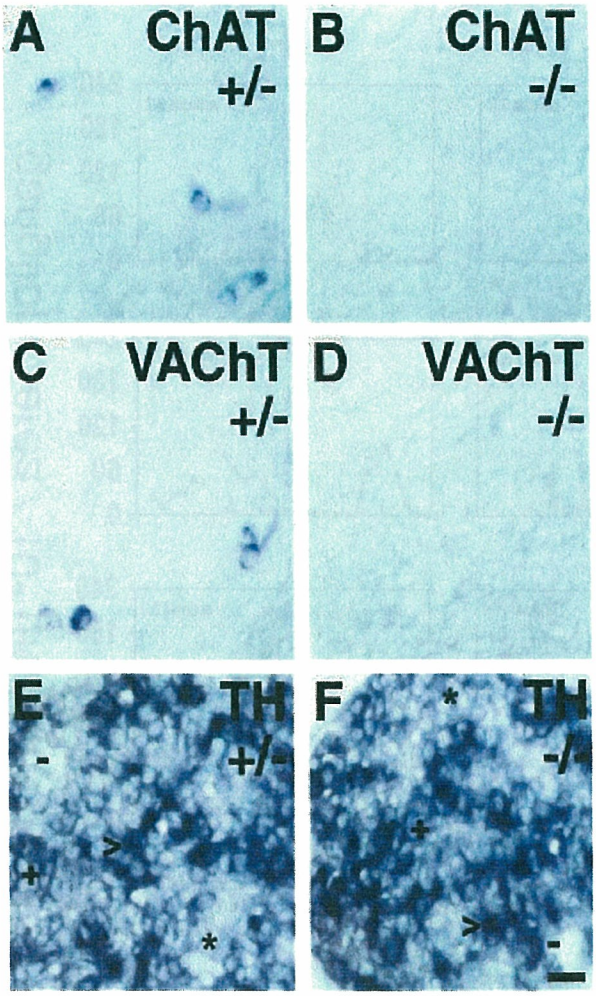

FIG. 3. Specific loss of cholinergic properties in stellate ganglia of homozygous c-ret mutant mice. Sections from heterozygous (+/–) and homozygous (–/–) c-ret mutant mice were hybridized with riboprobes for choline acetyltransferase (ChAT), the vesicular acetylcholine transporter (VAChT), and tyrosine hydroxylase (TH). In heterozygous animals, a small but distinct number of cells in stellate ganglia express detectable levels of ChAT (A) and VAChT (C). Such cells are almost entirely absent from homozygous mutant mice (B and D). TH expression is detectable in the vast majority of ganglionic cells in heterozygous (E) and homozygous (F) mutants. Expression levels differ strongly between cells such that TH-positive cells with strong (>), medium (+) and weak (*) expression were distinguished from TH-negative cells (–). Scale bar, 25 μm.

We first analysed by TH and DBH ISH the distribution of neurons in the region of the stellate ganglion along rostrocaudal levels and in relation to the thymus at E16. Similar to newborn animals, E16 wildtype and heterozygous mutant animals displayed ganglionic structures at the height of the thymus that were sharply demarcated cranially and partially fused with more caudally located, smaller nerve cell clusters (data not shown). The cranial end of the stellate ganglia was located close to the cranial end of the developing thymus in wildtype and heterozygous animals. In two out of three homozygous mutant animals, relatively large neuron aggregates were observed cranial to the thymus in addition to ganglionic structures at the level of the thymus. Whether the more cranially located cell clusters are misrouted superior cervical ganglion or stellate ganglion precursors, cannot be decided with certainty.

Quantitative analysis was performed for stellate ganglion size and cell number (Table 2) as described for newborn animals. Ganglionic volume in homozygous mutants appears reduced by 47% as compared to wildtype animals and the corresponding reduction in estimated ganglionic cell number amounts to 42%. In contrast to newborn animals, no significant difference in cell density is found. Also different from newborn animals, heterozygous animals show no significant alterations in ganglionic volume and cell number as compared to wildtype animals (Table 2).

Already at E16, c-ret mutation affects cholinergic properties in stellate ganglia (Fig. 7). ChAT mRNA signals are detectable in wildtype (Fig. 7A) and heterozygous (not shown) animals at low signal intensities. In homozygous c-ret mutants, ChAT-positive cells are largely missing (Fig. 7B). VAChT mRNA signals are stronger and positive cells are more numerous than ChAT-positive cells in the wildtype (Fig. 7C and E) and heterozygous (Fig. 7G) animals. In addition to strongly VAChT-positive cells, a fraction of cells, observed at E16 but not P0, express VAChT mRNA signals just above detection threshold (compare Fig. 7E and H). In homozygous c-ret mutants, cells with strong VAChT expression are largely absent (Fig. 7D and F) while weakly VAChT-positive cells are still detectable (Fig. 7F).

Quantitative analysis of ChAT-positive cells shows a highly significant reduction by 82% from 67.1 ± 17.2 cells per ganglion in wildtype animals to 11.9 ± 4.0 cells in homozygous mutants ($n \geq 5$ ganglia per genotype; ± SEM; $P = 0.008$, ANOVA). In heterozygous animals, the estimate of ChAT-positive cells is increased to 101.3 ± 10.3 cells per ganglion, which is due to a significantly enhanced density of ChAT-positive cells in heterozygous (73.9 ± 5.7/mm^2) as compared to wildtype animals (61.6 ± 9.3/mm^2) ($n = 10$ ganglia per genotype; $P < 0.05$, Mann–Whitney U-test).

Quantitative analysis of VAChT mRNA-positive cells is complicated by the variable detection of cells with expression levels just above background whose number was affected by the batches of riboprobe, alkaline phosphatase-conjugated antibody and colour substrate. In experiments ($n = 3$) showing only few low-intensity VAChT-positive cells (Fig. 7C and D), the estimate of VAChT mRNA-positive cells was 119 ± 26 (wildtype), 195 ± 20 (heterozygous), and 7 ± 0.5 (homozygous c-ret mutants) per ganglion ($n \geq 5$ ganglia per genotype; ± SEM). The reduction in the number of positive cells per ganglion by 94% in homozygous mutants is highly significant ($P = 0.001$, ANOVA) and is paralleled by a decrease in the density of VAChT-positive cells from 70 ± 19/mm^2 in wildtype to 9 ± 2/mm^2 in homozygous mutants. Interestingly, the number of VAChT-positive cells per ganglion in heterozygous mutants is increased to 164% of wildtype animals under such detection conditions, which is paralleled by an increase in the density of VAChT-positive cells to 121 ± 15/mm^2 in heterozygous animals ($n = 8$ (wildtype) and 14 (heterozygous) ganglia; $P < 0.05$, Mann–Whitney U-test). Experiments ($n = 3$) showing significant numbers of low-intensity VAChT-positive cells (as shown in Fig. 7E–G) yield an estimate of 469 ± 49 (wildtype), 367 ± 30 (heterozygous), and 192 ± 22 (homozygous c-ret mutants) VAChT-positive cells per ganglion ($n \geq 5$ ganglia per genotype; ± SEM). The 59% reduction between wildtype and homozygous mutant animals is highly significant ($P = 0.0004$, ANOVA) yet remains closer to the reduction in total cell number of mutant ganglia (42%) than to the reduction in ChAT-positive cells (82%). VAChT-positive cell numbers per ganglion from heterozygous animals are not significantly different from wildtype animals, similar to the number of ganglionic cells.

The decrease in ChAT and VAChT mRNA signals in homozygous c-ret mutant mice demonstrates the requirement of c-ret signalling for development of cholinergic neurons already at this embryonic stage. An

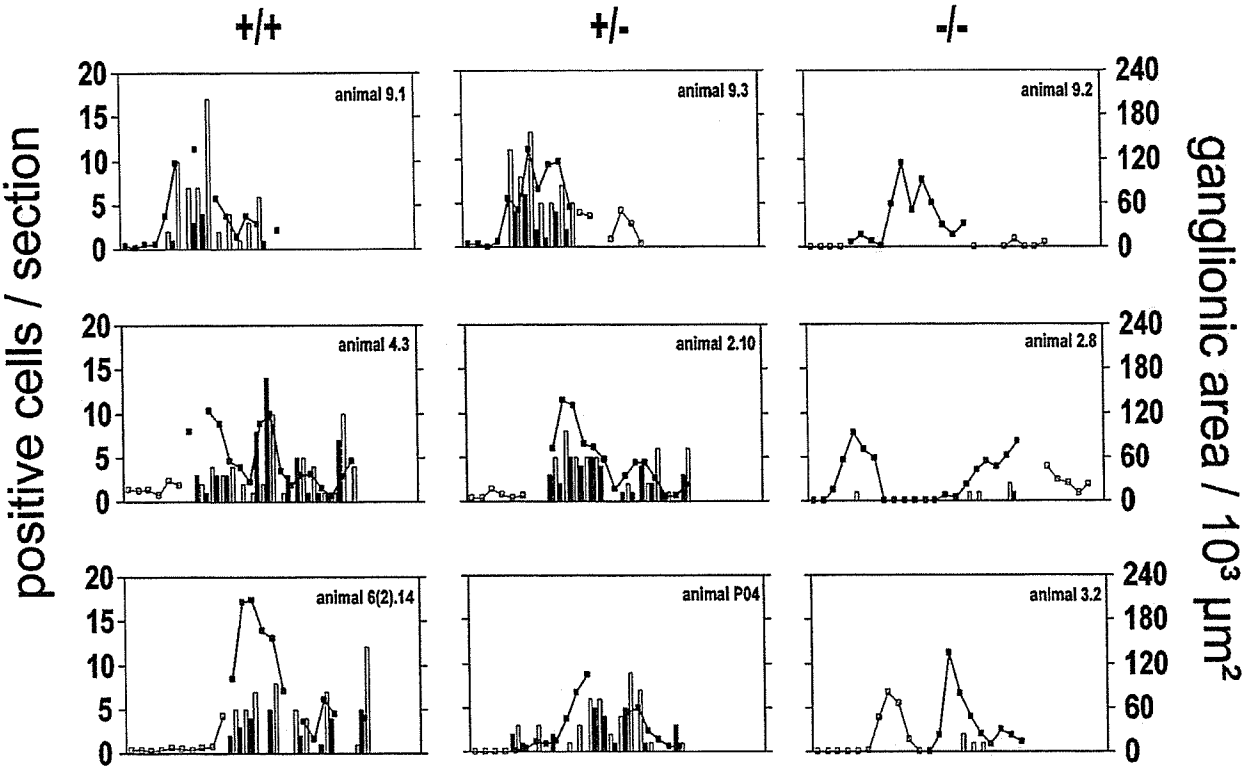

FIG. 4. Distribution of cholinergic cells in stellate ganglia of newborn wildtype and c-ret mutant mice. Serial sections from the ganglia shown in Fig. 1 are hybridized with ChAT and VAChT riboprobes. The numbers of ChAT (black bars) and VAChT (unfilled bars) positive cells are displayed against ganglionic area (black squares) for the respective section. Cell number and ganglionic area from the left and the right side in each section are pooled. Numbers of positive cells are given for each section where the ganglionic area is indicated by a black square. For sections where the ganglionic area is shown by a black square in the absence of unfilled or black bars, no ChAT or VAChT-positive cells were observed. Such sections are found very infrequently in wildtype and heterozygous ganglia whereas the vast majority of sections from homozygous mutants are devoid of detectable ChAT or VAChT expression. Unfilled squares show regions of the ganglia not analysed for ChAT or VAChT expression.

increase in density of ChAT and strongly VAChT-positive cells in heterozygous mutants indicates that c-ret action on cholinergic development may not be linearly related to gene dosage. This is not unprecedented as colonization of the colon by enteric neural crest cells in endothelin-3 mutant mice is more extensive in heterozygous c-ret mutant mice than c-ret wildtype animals (Barlow *et al.*, 2003). The presence of a weakly VAChT-positive cell population in E16 stellate ganglia complicated the quantitative analysis. The interesting observation that the effect of the c-ret mutation on this population barely exceeds the effect on the total ganglion cell number suggests that c-ret signalling is specifically required for enhanced expression of cholinergic markers.

Analysis of E13 and E14 embryos reveals that c-ret is not required for the initial induction of ChAT and VAChT mRNA expression

In order to investigate whether c-ret is necessary for the induction of cholinergic properties, we analysed E13 and E14 stellate ganglia. Previous studies had shown that VAChT mRNA is detectable at E12 in primary sympathetic ganglia and at E14 in secondary sympathetic ganglia of the rat (Schäfer *et al.*, 1997; Schütz *et al.*, 1998). As shown in Fig. 8, no overt difference was seen in VAChT and ChAT mRNA expression between stellate ganglia from E14 wildtype and c-ret homozygous or heterozygous mice. Expression levels were low and did not permit the precise determination of the numbers of positive neurons. Identical observations were made at E13. Together, these data suggest that c-ret is not essential for initiating the onset of VAChT and ChAT expression, but important for the subsequent expression of cholinergic markers at enhanced levels in a small subpopulation of stellate neurons.

Discussion

The present study provides evidence for a requirement of c-ret signal transduction for the development of cholinergic sympathetic neurons *in vivo*. Homozygous mutation of the c-ret kinase domain results in a massive loss of ChAT and VAChT mRNA in the mouse stellate ganglion. This effect becomes apparent during embryonic development (E16) when ChAT and VAChT become strongly expressed in a subset of sympathetic ganglion neurons. Before this time, expression of cholinergic properties is detectable at low levels and cannot be distinguished between wildtype and mutant mice. Thus, the data also demonstrate that c-ret kinase activity is not required for initial induction of expression from the cholinergic locus in sympathetic neurons but becomes necessary for development of cholinergic sympathetic neurons at more advanced developmental stages. Apparently, development of this neuron population is differently regulated at different stages as originally observed in the chick embryo (Ernsberger *et al.*, 1997; Geissen *et al.*, 1998; Duong *et al.*, 2002).

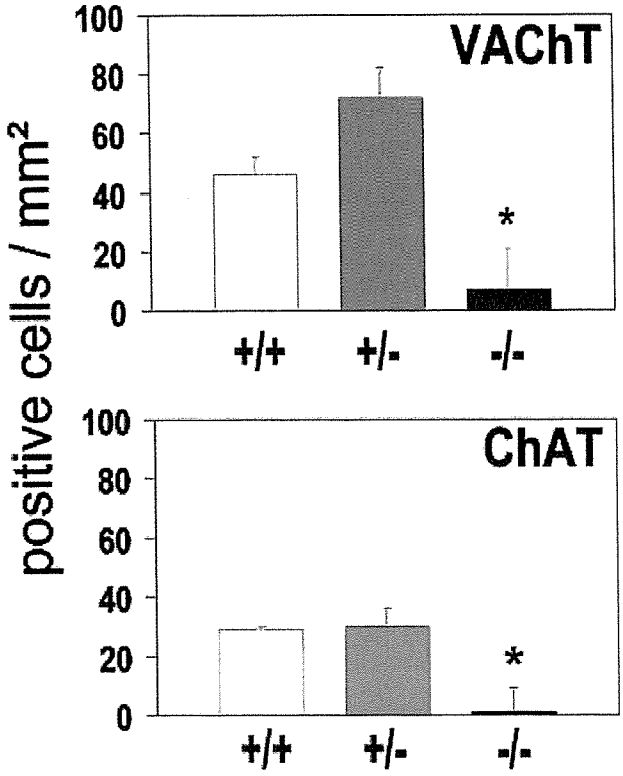

FIG. 5. The density of ChAT and VAChT-positive cells is reduced by more than 80% in homozygous c-ret mutant mice. The density of ChAT and VAChT-positive cells was determined in wildtype (+/+), heterozygous (+/–), and homozygous (–/–) c-ret mutant mice. For each genotype, three animals were analysed and for each animal at least four sections were counted. The bars show the mean number of positive cells per mm^2 ($n = 3$, ± SEM). The density of ChAT and VAChT-positive cells is significantly reduced in homozygous mutant mice ($^*P < 0.05$, Mann–Whitney and ANOVA) as compared to heterozygous and wildtype animals.

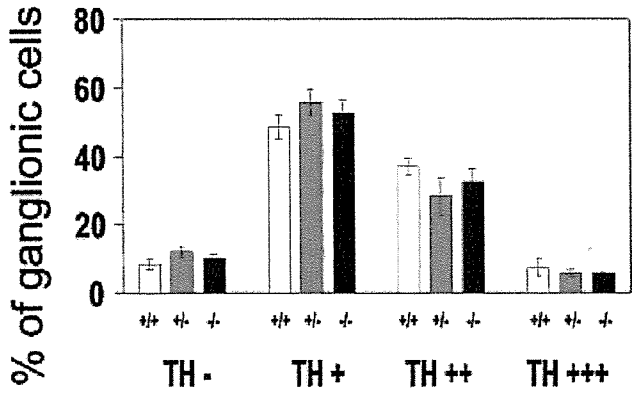

FIG. 6. The proportions of cells with different levels of TH expression are not affected by the c-ret mutation. The proportion of stellate ganglion neurons with strong (TH +++), medium (TH ++), weak (TH +), or no detectable (TH –) TH expression was determined in wildtype (+/+), heterozygous (+/–), and homozygous (–/–) ret mutants. At least three animals were analysed for each genotype and for each animal at least three sections of the stellate ganglia are counted. Numbers shown are means ± SEM. No statistically significant differences are observed when neuron classes are compared between the different genotypes (Mann–Whitney and ANOVA).

TABLE 2. Reduction of stellate ganglion size and cell number in E16 mice

Genotype	Ganglion volume (mm^3)	Cell density (per mm^2)	Cell number estimate (per ganglion)
+/+	0.038 ± 0.0032	5212 ± 620	9003 ± 1430
+/–	0.032 ± 0.0017	6262 ± 31	9254 ± 531
–/–	0.020 ± 0.0012**	5104 ± 174	5249 ± 509*

Ganglion volume and cell density were determined as described in Materials and methods. The cell numbers per ganglion were estimated by transforming the density per area into density per volume and correction by the Linderstrom-Lang/Abercrombie equation (Hedreen, 1998). Mean cell diameters used for correction were obtained from at least 60 cells per genotype: 9.6 μm, wildtype; 9.9 μm, heterozygous; 8.1 μm, homozygous mutants. Values given in the table are means ± SEM from five (wildtype), six (heterozygous), and four (homozygous) ganglia. Ganglion volume and total estimated cell number from wildtype and homozygous mutants are significantly different: $^*P < 0.05$, $^{**}P < 0.0005$ (ANOVA). No significant differences were observed between wildtype and heterozygous animals.

Several mechanisms may result in the reduced detection of cholinergic properties in c-ret mutant sympathetic ganglia. A loss of cholinergic neurons due to alterations of cell proliferation, cell migration, cell death, and effects on transcription from the cholinergic locus may account for the observed changes. As cholinergic neurons in the newborn mouse stellate ganglion amount to approximately 1% of total cells only, we cannot unequivocally favour or exclude any of the above possibilities.

Quantitative analysis of cell number (this study) as well as apoptotic figures (Enomoto *et al.*, 2001) indicates enhanced cell loss in stellate ganglia of newborn and embryonic c-ret mutant animals. As TH-positive cells amount to more than 90% of total ganglionic cells in newborn wildtype and mutant animals, the reduction in ganglionic cell number estimated to be 24% in c-ret mutants must include the catecholaminergic cell population. Thus, a role of c-ret signalling in cell survival may affect the number of catecholaminergic stellate cells. This cannot be easily extended to cholinergic VAChT and ChAT-positive cells, however. Even though the loss of cholinergic markers appears much more dramatic than the reduction in ganglion cell number and consequently catecholaminergic cells, the minute size of the cholinergic population cannot be expected to show significantly in ganglion cell estimates.

In fact, indirect evidence suggests an effect of c-ret signalling on expression of cholinergic properties rather than on survival of cholinergic cells. Increased apoptosis in newborn c-ret mutants does not occur preferentially in the cell population that expresses GFP from the *ret* locus (Enomoto *et al.*, 2001). These cells correspond to ret-positive cells in wildtype animals and, surprisingly, appear nonoverlapping with the dying cells in mutant sympathetic ganglia. Indeed, the proportion of GFP-positive cells in newborn stellate ganglia is almost identical between heterozygous and homozygous mutant animals (Enomoto *et al.*, 2001). As c-ret is coexpressed with cholinergic properties in chick sympathetic ganglia (Ernsberger *et al.*, 2000), these observations suggest that cells of the cholinergic population persist in c-ret mutant animals without expression of wildtype levels of cholinergic markers VAChT and ChAT. Due to comparatively low levels of VAChT and ChAT expression already in stellate ganglia of wildtype mice, coexpression analysis between cholinergic markers and c-ret could neither be performed on RNA nor on protein level (U.E., unpublished observations) to directly strengthen this conclusion.

Taken together, homozygous c-ret mutation reduces ganglionic cell number estimates by more than 40% at E16 and more than 20% at P0. This may result from survival effects of c-ret signalling, even though

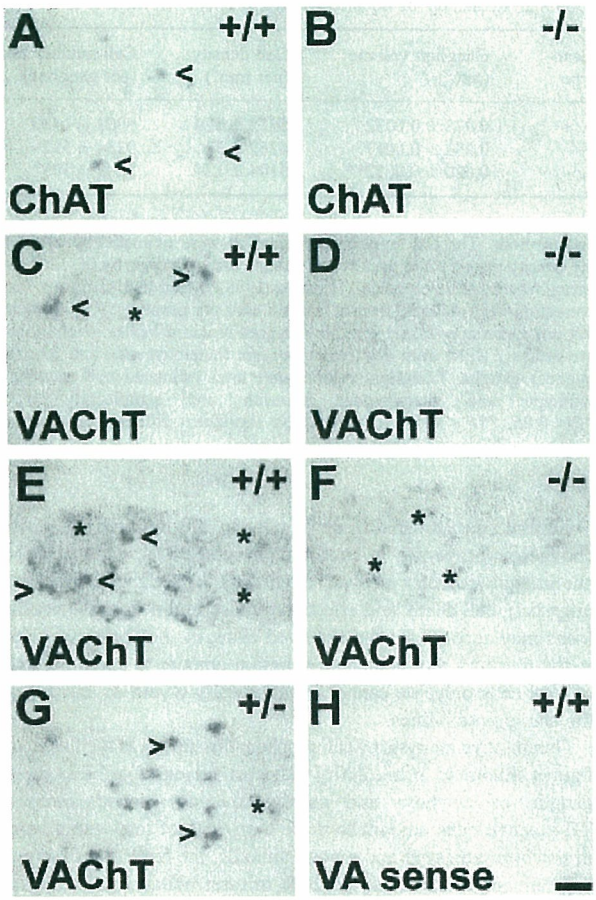

FIG. 7. Reduction of ChAT and VAChT mRNA signals in stellate ganglia of c-ret mutant mice at embryonic day 16. Sections from wildtype (+/+), heterozygous (+/–) and homozygous (–/–) c-ret mutant mice were hybridized with riboprobes for choline acetyltransferase (ChAT) and the vesicular acetylcholine transporter (VAChT). Cells with weak ChAT signals (<) are found in wildtype animals (A), whereas homozygous mutants are largely devoid of ChAT-positive cells (B). Cells with relatively strong VAChT signals (< >) are detected in wildtype (C and E) and heterozygous (G) animals but absent from homozygous c-ret mutants (D and F). Depending on the batch of riboprobe, alkaline phosphatase-conjugated antibody, and colour substrate, cells with weak VAChT signals (*) can be detected in both wildtype (E) and homozygous mutants (F). Comparison with sense riboprobe (H) shows that low intensity signals are above background. Panels C and D show results obtained with one batch of solutions, panels E–H were obtained with different solutions. Scale bar, 50 μm.

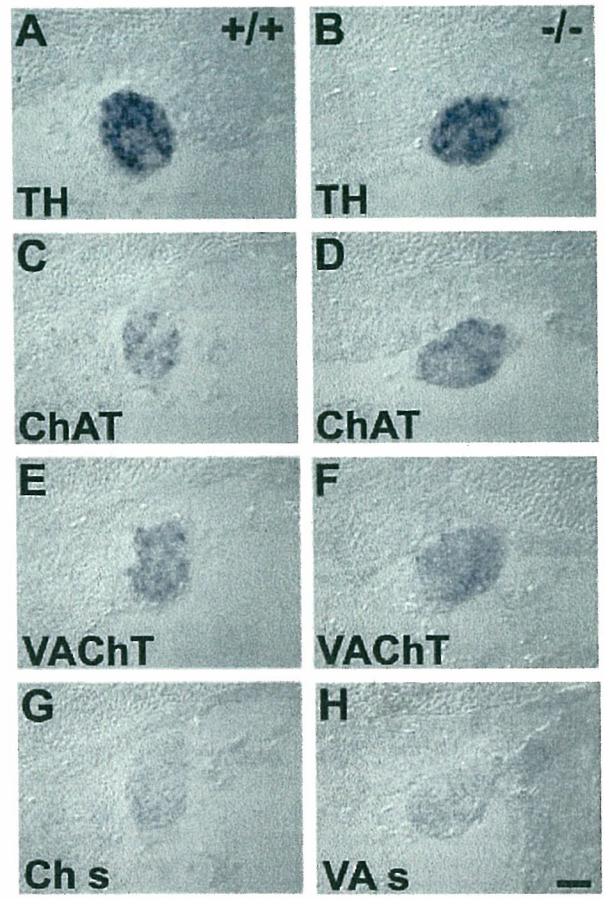

FIG. 8. ChAT and VAChT are expressed at low levels in sympathetic ganglia of 14-day-old wildtype and ret mutant mice. Sections from wildtype (+/+) and homozygous (–/–) c-ret mutant mice were hybridized with antisense riboprobes for tyrosine hydroxylase (TH) (A and B), choline acetyltransferase (ChAT) (C and D), the vesicular acetylcholine transporter (VAChT) (E and F), as well as sense riboprobes for ChAT (G) and VAChT (H). TH expression allows localization of sympathetic ganglia (A and B). ChAT (C and D) and VAChT (E and F) mRNAs are detectable in wildtype and homozygous mutant animals at low expression levels. Sense riboprobes for ChAT (G) and VAChT (H) give no signal and demonstrate that the weak signals detected with the antisense riboprobes are clearly above background. Scale bar, 50 μm.

effects on proliferation and migration cannot be excluded. A specific reduction by more than 80–90% of ChAT and VAChT-positive cells is observed at P0 and at E16, at least for cells with high expression levels. The mechanism of this reduction is currently unclear even though indirect evidence favours an effect on gene expression rather than cell death. Whether the effects of c-ret on total cell number and on ChAT and VAChT-positive cells are mediated by the same or by different ligands and alpha receptor subunits, remains to be determined.

Both ChAT and VAChT are expressed from the cholinergic gene locus in several animal species where the coding sequence for VAChT is located in the first intron of the ChAT gene (Eiden, 1998). The regulation of expression by common promoter elements is considered responsible for the coexpression of both genes even though differences in relative expression have been reported in rat development (Holler *et al.*, 1996; Schütz *et al.*, 2001).

In our study, numbers of VAChT-positive cells are consistently higher than ChAT-positive cells. As VAChT ISH signals tend to be higher than ChAT signals in sympathetic neurons, we suspect VAChT mRNA levels to be higher than ChAT mRNA levels. A similar observation is made in chick sympathetic ganglia (U.E., unpublished observations) and the rat peripheral nervous system (Schütz *et al.*, 2001). It is hypothesized that such observations may be explained by usage of different promoters in the cholinergic gene locus. Consequently, ChAT mRNA could be expressed in some VAChT-positive cells below ISH detection threshold. This suggests that VAChT is the more sensitive marker for cholinergic gene expression and differentiation, at least for analysis in the peripheral nervous system. Compared to immunohistochemistry (IHC) for VAChT (Stanke *et al.*, 2000), ISH provides more sensitive detection due to higher signal-to-background ratios and the absence of signals from fibers and terminals that may obscure faint staining of ganglionic cell bodies.

Despite the limitation of histological methods such as ISH by detection thresholds, altered cholinergic transmission in sweat glands of GFRalpha2 mutant mice (Hiltunen & Airaksinen, 2002) supports the conclusion that the effect of c-ret signalling on ChAT and VAChT expression may affect cholinergic neurotransmission.

Whether c-ret acts directly or indirectly is an important question to be resolved. It has been demonstrated that outgrowth of sympathetic fibers is compromised in c-ret mutants (Enomoto *et al.*, 2001) as well as GFRalpha3 and artemin mutants (Nishino *et al.*, 1999; Honma *et al.*, 2002). As expression of cholinergic properties in a subpopulation of sympathetic neurons innervating rodent sweat glands is a consequence of interaction with target tissues (reviewed in Landis, 1990; Ernsberger & Rohrer, 1999), c-ret mutation may act via interfering with target innervation. Thus, target-derived cholinergic differentiation factors may not access neurons in mutant animals. As some SCG neurons encounter their peripheral targets already at E15.5 (Fagan *et al.*, 1996) this may also be the case for stellate neurons even though the time of innervation of peripheral targets by mouse stellate neurons is currently not known. Neurokine growth factors were, for a long time, hypothesized to act as cholinergic differentiation factors in sweat glands (Rohrer, 1992; Habecker *et al.*, 1997). Thus, lack of c-ret signalling may alter neurite outgrowth and prevent access of sympathetic neurons to neurokines in the target tissues. Alternatively, GDNF family ligands may act directly. Indeed, neurturin is detectable in mouse sweat glands (Hiltunen & Airaksinen, 2002) and may directly affect cholinergic differentiation.

In addition, growth factors along the neurite outgrowth paths may also play a role. The demonstration of artemin expression along embryonic blood vessels (Honma *et al.*, 2002) provokes the question of whether signalling along this outgrowth pathway for sympathetic neurites may contribute to cholinergic development either by promoting target access or by directly affecting expression from the cholinergic gene locus. The complex regulation of c-ret and GFRalphas during embryogenesis at least in the SCG (Nishino *et al.*, 1999) indicates that GDNF family ligands may exert multiple functions in sympathetic neuron development.

In summary, we have shown that c-ret is not required for the initial induction of cholinergic properties in sympathetic neurons. c-ret activity, however, is indispensable for cholinergic sympathetic neurons at later embryonic and postnatal stages. As we show, to our knowledge for the first time, the requirement of a specific signalling system for normal development of ChAT and VAChT-positive neurons in embryonic and newborn sympathetic ganglia, a number of questions arises. Is the moderate reduction of ganglionic cell number and the massive reduction of ChAT and VAChT-positive cells in c-ret mutants due to interference with signalling from one or from different c-ret ligands? Is the underlying mechanism the same, i.e. cell death, or are several functions such as proliferation, cell death, and gene expression affected? In addition, the question remains to be settled as to whether c-ret acts directly or indirectly, for example by promoting access to target-derived cholinergic differentiation factors and/or survival factors. Irrespective of the answers to these questions, the massive and specific effect of c-ret mutation on ChAT and VAChT-positive cells in stellate ganglia establishes c-ret signalling as a key player in transmitter phenotype diversification of sympathetic neurons.

Acknowledgements

We wish to thank V. Pachnis (National Institute for Medical Research, London, UK) and M. Saarma (Institute of Biotechnology, Helsinki, Finland) for kindly providing c-ret mutant mice. We are thankful to J.K. Blusztajn (Boston University, Boston, MA), J.F. Brunet and C. Goridis (Ecole Normale Superieure, Paris, France) for making mouse cDNAs available. Alexandra Allmendinger is acknowledged for help with preparing animals and genotyping. We thank Oliver von Bohlen und Halbach (IZN, Heidelberg, Germany) for advice on cell number analysis and Hermann Rohrer (Max-Planck-Institut for Brain Research, Frankfurt, Germany) for critical suggestions on the manuscript. B.B. is supported by the National Institute of Health (NIH grant NS44238). K.B. and U.E. are supported by the Deutsche Forschungsgemeinschaft (DFG grant ER 145/4 to UE).

Abbreviations

ChAT, choline acetyltransferase; DBH, dopamine β-hydroxylase; E, embryonic day; ISH, *in situ* hybridization; TH, tyrosine hydroxylase; VAChT, vesicular acetylcholine transporter.

References

Airaksinen, M.S. & Saarma, M. (2002) The GDNF family: signalling, biological functions and therapeutic value. *Nature Rev. Neurosci.*, **3**, 383–394.

Allmendinger, A., Stoeckel, E., Saarma, M., Unsicker, K. & Huber, K. (2003) Development of adrenal chromaffin cells is largely normal in mice lacking the receptor tyrosine kinase c-Ret. *Mech. Dev.*, **120**, 299–304.

Barlow, A., de Graaff, E. & Pachnis, V. (2003) Enteric nervous system progenitors are coordinately controlled by the G protein-coupled receptor EDNRB and the receptor tyrosine kinase RET. *Neuron*, **40**, 905–916.

Brodski, C., Schaubmar, A. & Dechant, G. (2002) Opposing functions of GDNF and NGF in the development of cholinergic and noradrenergic sympathetic neurons. *Mol. Cell. Neurosci.*, **19**, 528–538.

Brodski, C., Schnurch, H. & Dechant, G. (2000) Neurotrophin-3 promotes the cholinergic differentiation of sympathetic neurons. *Proc. Natl Acad. Sci. USA*, **97**, 9683–9688.

Burau, K., Huber, K., Allmendinger, A., Misawa, H., Berse, B., Blusztajn, J.K., Saarma, M., Unsicker, K. & Ernsberger, U. (2002) c-ret signaling and cholinergic differentiation of sympathetic neurons. *Soc. Neurosci. Abstr.*, 231.11.

Byrkit, D.R. (1987) *Statistics Today.* Benjamin/Cummings, Menlo Park, CA.

Duong, C.V., Geissen, M. & Rohrer, H. (2002) The developmental expression of vasoactive intestinal peptide (VIP) in cholinergic sympathetic neurons depends on cytokines signaling through LIFRbeta-containing receptors. *Development*, **129**, 1387–1396.

Durbec, P.L., Larsson-Blomberg, L.B., Schuchardt, A., Costantini, F. & Pachnis, V. (1996) Common origin and developmental dependence on c-ret of subsets of enteric and sympathetic neuroblasts. *Development*, **122**, 349–358.

Eiden, L.E. (1998) The cholinergic gene locus. *J. Neurochem.*, **70**, 2227–2240.

Enomoto, H., Crawford, P.A., Gorodinsky, A., Heuckeroth, R.O., Johnson, E.M. Jr & Milbrandt, J. (2001) RET signaling is essential for migration, axonal growth and axon guidance of developing sympathetic neurons. *Development*, **128**, 3963–3974.

Ernsberger, U. (2000) Evidence for an evolutionary conserved role of BMP growth factors and Phox2 transcription factors during noradrenergic differentiation of sympathetic neurons: induction of a putative synexpression group of neurotransmitter-synthesizing enzymes. *Eur. J. Biochem.*, **267**, 6976–6981.

Ernsberger, U. (2001) The development of postganglionic sympathetic neurons: coordinating neuronal differentiation and diversification. *Auton. Neurosci.*, **94**, 1–13.

Ernsberger, U., Patzke, H. & Rohrer, H. (1997) The developmental expression of choline acetyltransferase (ChAT) and the neuropeptide VIP in chick sympathetic neurons: evidence for different regulatory events in cholinergic differentiation. *Mech. Dev.*, **68**, 115–126.

Ernsberger, U., Reissmann, E., Mason, I. & Rohrer, H. (2000) The expression of dopamine β-hydroxylase, tyrosine hydroxylase, and Phox2 transcription factors in sympathetic neurons: evidence for common regulation during noradrenergic induction and diverging regulation later in development. *Mech. Dev.*, **92**, 169–177.

Ernsberger, U. & Rohrer, H. (1999) The development of the cholinergic neurotransmitter phenotype in postganglionic sympathetic neurons. *Cell Tiss. Res.*, **297**, 339–361.

Fagan, A.M., Zhang, H., Landis, S., Smeyne, R.J., Silos-Santiago, I. & Barbacid, M. (1996) TrkA, but not TrkC, receptors are essential for survival of sympathetic neurons *in vivo*. *J. Neurosci.*, **16**, 6208–6218.

Geissen, M., Heller, S., Pennica, D., Ernsberger, U. & Rohrer, H. (1998) The specification of sympathetic neurotransmitter phenotype depends on gp130 cytokine receptor signaling. *Development*, **125**, 4791–4801.

Goridis, C. & Rohrer, H. (2002) Specification of catecholaminergic and serotonergic neurons. *Nature Rev. Neurosci.*, **3**, 531–541.

Habecker, B.A., Symes, A.J., Stahl, N., Francis, N.J., Economides, A., Fink, Y.S., Yancopoulos, G.D. & Landis, S.C. (1997) A sweat gland-derived differentiation activity acts through known cytokine signaling pathways. *J. Biol. Chem.*, **272**, 30421–30428.

Hedreen, J.C. (1998) What was wrong with the Abercrombie and empirical cell counting methods? A review. *Anat. Rec.*, **250**, 373–380.

Hiltunen, P.H. & Airaksinen, M.S. (2002) Deficient sympathetic cholinergic innervation to sweat glands in mice lacking GFR2. *Soc. Neurosci. Abstr.*, 428.17.

Holler, T., Berse, B., Cermak, J.M., Diebler, M.F. & Blusztajn, J.K. (1996) Differences in the developmental expression of the vesicular acetylcholine transporterand choline acetyltransferase in the rat brain. *Neurosci. Lett.*, **212**, 107–110.

Honma, Y., Araki, T., Gianino, S., Bruce, A., Heuckeroth, R., Johnson, E. & Milbrandt, J. (2002) Artemin is a vascular-derived neurotropic factor for developing sympathetic neurons. *Neuron*, **35**, 267–282.

Huber, K., Bruhl, B., Guillemot, F., Olson, E.N., Ernsberger, U. & Unsicker, K. (2002) Development of chromaffin cells depends on MASH1 function. *Development*, **129**, 4729–4738.

Ishii, K., Oda, Y., Ichikawa, T. & Deguchi, T. (1990) Complementary DNAs for choline acetyltransferase from spinal cords of rat and mouse: nucleotide sequences, expression in mammalian cells, and *in situ* hybridization. *Brain. Res. Mol. Brain. Res.*, **7**, 151–159.

Landis, S.C. (1990) Target regulation of neurotransmitter phenotype. *TINS*, **13**, 344–350.

Nishino, J., Mochida, K., Ohfuji, Y., Shimazaki, T., Meno, C., Ohishi, S., Matsuda, Y., Fujii, H., Saijoh, Y. & Hamada, H. (1999) GFR alpha3, a component of the artemin receptor, is required for migration and survival of the superior cervical ganglion. *Neuron*, **23**, 725–736.

Robertson, K. & Mason, I. (1995) Expression of ret in the chicken embryo suggests roles in regionalisation of the vagal neural tube and somites and in development of multiple neural crest and placodal lineages. *Mech. Dev.*, **53**, 329–344.

Rohrer, H. (1992) Cholinergic neuronal differentiation factors: evidence for the presence of both CNTF-like and non-CNTF-like factors in developing rat footpad. *Development*, **114**, 689–698.

Schäfer, M.K.H., Eiden, L.E. & Weihe, E. (1997) Cholinergic neurons and terminal fields revealed by immunohistochemistry for the vesicular acetylcholine transporter. II. The peripheral nervous system. *Neuroscience*, **84**, 361–376.

Schotzinger, R., Yin, X. & Landis, S.C. (1994) Target determination of neurotransmitter phenotype in sympathetic neurons. *J. Neurobiol.*, **25**, 620–639.

Schuchardt, A., D'Agati, V., Larsson-Blomberg, L., Costantini, F. & Pachnis, V. (1994) Defects in the kidney and enteric nervous system of mice lacking the tyrosine kinase receptor Ret. *Nature*, **367**, 380–383.

Schütz, B., Schäfer, M.K.H., Eiden, L.E. & Weihe, E. (1998) Vesicular amine transporter expression and isoform selection in developing brain, peripheral nervous system, and gut. *Dev. Brain Res.*, **106**, 181–204.

Schütz, B., Weihe, E. & Eiden, L.E. (2001) Independent patterns of transcription for the products of the rat cholinergic gene locus. *Neuroscience*, **104**, 633–642.

Stanke, M., Geissen, M., Götz, R., Ernsberger, U. & Rohrer, H. (2000) The early expression of VAChT and VIP in mouse sympathetic ganglia is not induced by cytokines acting through LIFRβ or CNTFRα. *Mech. Dev.*, **91**, 91–96.

European Journal of Neuroscience, Vol. 19, pp. 3129–3141, 2004

The LIM homeobox gene, *L3/Lhx8*, is necessary for proper development of basal forebrain cholinergic neurons

Tetsuji Mori,[1] Zhang Yuxing,[1,2] Hiromi Takaki,[1] Mayumi Takeuchi,[1] Ken Iseki,[1,2] Seita Hagino,[1,3] Jun-ichi Kitanaka,[4] Motohiko Takemura,[4] Hidemi Misawa,[5] Masahito Ikawa,[6] Masaru Okabe[6] and Akio Wanaka[7]
[1]Department of Cell Science, Institute of Biomedical Sciences,
[2]Department of Anesthesiology, and [3]Department of Orthopedic Surgery, Fukushima Medical University, 1 Hikarigaoka, Fukushima City, Fukushima, 960-1295 Japan
[4]Department of Pharmacology, Hyogo College of Medicine, 1–1 Mukogawa, Nishinomiya City, Hyogo, 663-8501 Japan
[5]Department of Neurology, Tokyo Metropolitan Institute for Neuroscience, 2–6 Musashidai, Fuchu City, Tokyo, 183-8526 Japan
[6]Genome Information Research Center, Osaka University, 3–1 Yamadaoka, Suita City, Osaka, 565-0871 Japan
[7]Department of Anatomy, Nara Medical University, 840 Shijo-cho, Kashihara City, Nara, 634-8521 Japan

Keywords: mouse, null mutant, LIM domain, brain, choline acetyltransferase, transcription factor

Abstract

Basal forebrain cholinergic neurons (BFCNs) are involved in cognitive functions such as learning and memory, and are affected in several neurodegenerative diseases (e.g. Alzheimer's disease). Despite their importance, the molecular mechanisms of their development are not fully elucidated. A recent report demonstrated that some BFCNs in adult rat are positive for L3/Lhx8, a LIM homeobox transcription factor. To examine the function of L3/Lhx8 in the development of BFCNs, we generated *L3/Lhx8* gene-disrupted mice. In these mice, cells expressing cholinergic neuron markers, such as choline acetyltransferase, vesicular acetylcholine transporter and p75 low-affinity NGF receptor, were markedly reduced in the basal forebrain, whereas other cholinergic neurons including brain stem and spinal motor neurons expressed the markers. Neurotransmitter phenotypes other than cholinergic in the basal forebrain appeared intact. From these results, we suggested that L3/Lhx8 has a pivotal and specific role in the development and/or maintenance of BFCNs.

Introduction

Cholinergic neurons in the basal forebrain (BFCNs) have been extensively studied in several species of mammals and accumulating evidence indicates that they play important roles in arousal, attention, learning and memory (Everitt & Robbins, 1997). They are affected in several neurodegenerative disorders such as Huntington's disease (Ferrante *et al.*, 1987) and Alzheimer's disease (Whitehouse *et al.*, 1982). In spite of their importance in cognitive functions, the molecular mechanisms of their normal development and of degeneration in the above-mentioned disorders have not been fully elucidated.

Transcription factors regulate neurotransmitter phenotypes with sequential and combinatorial expression patterns (Goridis & Brunet, 1999); recent studies have demonstrated that certain transcription factors were crucial in such regulation. For example, Nurr1, an orphan nuclear receptor, is essential for the expression of the dopaminergic phenotype in the midbrain (Saucedo-Cardenas *et al.*, 1998). This requirement is specific to the midbrain dopaminergic neurons, because other populations with dopaminergic phenotype develop normally in the absence of the gene (Zetterstrom *et al.*, 1997). Serotonergic neurons in the hindbrain require a LIM-homeobox (Lhx) transcription factor Lmx1b for their proper development (Cheng *et al.*, 2003; Ding *et al.*, 2003). These transcription factors are characteristically expressed in their corresponding neurons.

Many transcription factors are expressed in the developing basal forebrain and gene-disrupted mice exhibit malformation of the forebrain (Kimura *et al.*, 1996; Casarosa *et al.*, 1999; Hallonet *et al.*, 1999; Sussel *et al.*, 1999; Toresson *et al.*, 2000; Yun *et al.*, 2001). However, BFCNs were not affected in these mice. Among the transcription factors, *L3/Lhx8* is specifically co-expressed with *Gbx1* in the adult rat BFCNs (Asbreuk *et al.*, 2002), suggesting its possible implication in development of BFCNs by analogy to the *Nurr1* or *Lmx1b* cases. Zhao *et al.* (1999) generated *L3/Lhx8*-deficient mice and reported that these mice exhibited a cleft palate, but they did not discuss the phenotype of their brains. A notable point in that study is that a complete cleft of the secondary palate occurred in only 60% of the homozygous mice. They supposed that in these knock-out mice *Lhx6* might partially compensate for the *L3/Lhx8* function (Zhao *et al.*, 1999), because L3/Lhx8 and Lhx6 share about 60% amino acid sequence similarity and the distribution of L3/Lhx8 mRNA-positive cells in the embryo significantly overlapped with those expressing *Lhx6* (Grigoriou *et al.*, 1998; Kimura *et al.*, 1999; Zhao *et al.*, 1999; Zhang *et al.*, 2002). Taken together, a different knock-out strategy would be required to circumvent the potential compensation by Lhx6 *in vivo*.

The LIM domain of Lhx transcription factors is a protein–protein interaction domain that is necessary for binding with Ldbs, co-factors for the transcriptional activity of Lhx proteins (Dawid *et al.*, 1998). This domain, when overexpressed *in vivo*, could function as a

Correspondence: Dr A. Wanaka, as above.
E-mail: akiow@naramed-u.ac.jp

Received 25 March 2004, accepted 2 April 2004

doi:10.1111/j.1460-9568.2004.03415.x

dominant negative form that could sequester Ldbs (Taira *et al.*, 1994; Kikuchi *et al.*, 1997; O'Keefe *et al.*, 1998; Segawa *et al.*, 2001). As an attempt to curtail *Lhx6* compensation, we generated another line of L3/Lhx8-deficient mice in which the LIM domains of L3/Lhx8 were expressed from the recombinant allele. The LIM domain protein could serve as a dominant negative form to limit Lhx6 functions in the *L3/Lhx8*-targeted cells. Hereafter, we call these δHD/δHD mice to distinguish them from the previously generated *L3/Lhx8−/−* mice (Zhao *et al.*, 1999). The gross morphology and molecular marker expression of the developing basal forebrain in our δHD/δHD mice were normal; the only defect we identified in the brain was marked reduction of BFCNs.

Methods

Construction of the L3/Lhx8 *targeting vector*

In order to knock out the *L3/Lhx8* gene and simultaneously to produce a putative dominant-negative form of the L3/Lhx8 protein, we aimed at exon7 of the *L3/Lhx8* gene, which encodes the core region of the homeodomain (see Fig. 2a). About 7 kbp genomic DNA fragment flanking the exon7 was subcloned in pBlueskript-KS(+). Exon7 was replaced by a *PGK-Neo* cassette in the inverted orientation and at both ends of the targeting vector *MC1-DTA* cassettes were added. In addition, a '*SIGP*' cassette was inserted downstream of the *PGK-Neo* cassette. '*SIGP*' cassette stands for *Splicing Acceptor* + *IRES* (internal ribosomal entry site) + *GFP* (green fluorescent protein) + *PolyA* signal (see Fig. 2a). By inserting this cassette in the targeting vector, the truncated *L3/Lhx8* mRNA (from the exon1 to the exon6) and the *IRES–GFP–PolyA signal* fusion mRNA can be expressed under control of the *L3/Lhx8* promoter, and from this fusion mRNA, the GFP protein could be translated via *IRES* (see Fig. 2c and d). All animal experiments were carried out in accordance with the regulations of the Animal Care and Use Committee of Nara University. For harvesting tissues, animals were killed under deep anaesthesia with pentobarbital.

Generation of L3/Lhx8 *δHD/δHD mice and genotyping*

A D3 ES cell was maintained on mitomycin C-treated G418-resistant mouse embryonic fibroblasts (Harada *et al.*, 1999). ES cells (1.0×10^7) suspended in PBS(–) were electroporated (240 V, 500 μF, about 6.0–7.0 ms) with NotI-digested *L3/Lhx8*-targeted vector. Twenty four hours after the electroporation, G418 was added to the medium (2 μM) and G418-resistant clones were selected. A total of 144 individual clones were picked up and screened for homologous recombination by the PCR method; the forward primer was 5′-AGGGGTATGGCTA-CAGTTGTATCTC-3′ and the reverse primer was 5′-CAGCAG-CCTCTGTTCCACATACACT-3′. After the PCR screening, final confirmation of the homologous recombination was performed by Southern blot analysis. A 5′ probe recognized a 3.0-kbp fragment of the wild-type allele and a 10.0-kbp fragment of recombinant allele digested with *Eco*RI, and a 3′ probe recognized a 7.0-kbp fragment of the wild-type allele and a 10.0-kbp fragment of recombinant allele digested with *Eco*RV (see Fig. 2b). We obtained six independent targeted disrupted ES clones. Four out of six clones were chosen and injected into blastocysts derived from C57BL/6 to produce chimeric mice.

Chimeric pups were identified by their agouti coat colour. Chimeric males were bred to C57Bl/6J females and germline transmission was determined by the coat colour of the offspring. Genotyping of progeny was carried out by Southern blotting of tail or placental biopsy genomic DNA, as mentioned above. As a result, two independent lines of δHD/δHD mice were produced and they exhibited the same phenotype. For timed pregnancies, we designated E0.5 as 12:00 h when the morning vaginal plugs were identified.

Histological analysis and cell counting

To characterize and compare brain phenotypes of wild-type (WT), heterozygotes and homozygotes, genotyped embryos, newborn pups and young adults were subjected to *in situ* hybridization or immunocytochemistry. All embryos used in this study were immersion-fixed in 4% paraformaldehyde/PBS at 4 °C. Subsequently, they were cryo-protected in 30% sucrose before sectioning at 12 μm on a cryostat. Newborn pups and young adults were perfused transcardially with 4% paraformaldehyde/PBS and brains dissected out and post-fixed with the same fixative. Brains were then cryo-protected in 30% sucrose/PBS and sectioned at 12 μm on a cryostat. Embryonic brains were examined with *in situ* hybridization using gene probes that can characterize basal forebrain structures. Brains of pups and young adults were checked primarily for neurotransmitter phenotypes using *in situ* hybridization or immunocytochemistry.

To compare the cholinergic phenotypes of young adult brains (+/+, δHD/+, δHD/δHD) in detail, the BFCNs were counted. Three animals for each genotype were perfusion-fixed and serial brain sections were subjected to choline acetyltransferase (ChAT) immunohistochemistry. To avoid any counting bias, we first defined the anteroposterior extension of each nucleus (e.g. from Bregma +1.34 mm to Bregma +0.74 mm for the vertical limb of the diagonal band nucleus) according to the mouse brain atlas of Paxinos & Franklin (2001). Five sections were selected from the extension at regular intervals (e.g. 120-μm intervals for the vertical limb of the diagonal band nucleus) and ChAT-positive cells in the sections were counted.

In situ *hybridization*

In situ hybridization (ISH) and double-labelling fluorescence ISH was performed as described previously (Nikaido *et al.*, 2001; Iseki *et al.*, 2002). cDNA probe templates for ISH and their providers are listed below. EST clones were used after their nucleotide sequences were confirmed, and their gene bank accession numbers were indicated.

Nkx2.1, *Dlx-1*, *Dlx-2* and *Dlx-5* (kind gift of Dr J. L. Rubenstein, UCSF); *L3/Lhx8* (Matsumoto *et al.*, 1996); *Lhx6* (kind gift of Dr T. Taga, Kumamoto University) (Kimura *et al.*, 1999); *Gbx-2* (isolated with PCR: forward primer: ATGAGCGCAGCGTTCCCGCCGTCG-CT, reverse primer: CCGTCGACTGCACTCAACTCAAAAAGCC); *shh* (kind gift of Dr M. Nakafuku, University of Tokyo); *patched* (Acc. No. aa080038) (Tojo *et al.*, 1999); *smoothened* (Tojo *et al.*, 1999); *vesicular acetylcholine transporter* (VAChT; Misawa *et al.*, 2001); *GAD67* (Acc. No. W59173), *substance P* (Acc. No. AA982788); *enkephalin* (Acc. No. AA117032); *somatostatin* (Acc. No. AA051655); *neuropeptide Y* (Acc. No. W70782).

Double-staining of fluorescence *in situ* hybridization (FISH) was performed with an FITC-labelled *L3/Lhx8* cRNA probe and digoxygenin-labelled *Lhx6* cRNA, as described previously (Iseki *et al.*, 2002).

Immunohistochemistry

The antibodies used were: anti-GABA antibody (Sigma A2052), anti-ChAT and anti-CHT-1 (Misawa *et al.*, 2001), and anti-p75 NGF receptor (Chemicon AB1554).

RT-PCR

Total RNA was prepared from E14.5 embryonic basal forebrain, excluding the cerebral cortex, with TRIzol (Invitrogen), and was treated with DNaseI. Oligo-dT primed cDNA was synthesized with